IOWA STATE UNIVERSITY
Digital Repository

Retrospective Theses and Dissertations | Iowa State University Capstones, Theses and Dissertations

2003

Ultra-thin alumina barrier magnetic tunnel junctions

Bryan Kent Oliver
Iowa State University

Follow this and additional works at: https://lib.dr.iastate.edu/rtd

Part of the Electrical and Electronics Commons

Recommended Citation

Oliver, Bryan Kent, "Ultra-thin alumina barrier magnetic tunnel junctions " (2003). *Retrospective Theses and Dissertations*. 1454.
https://lib.dr.iastate.edu/rtd/1454

This Dissertation is brought to you for free and open access by the Iowa State University Capstones, Theses and Dissertations at Iowa State University Digital Repository. It has been accepted for inclusion in Retrospective Theses and Dissertations by an authorized administrator of Iowa State University Digital Repository. For more information, please contact digirep@iastate.edu.

المنارة للاستشارات

www.manaraa.com

Ultra-thin alumina barrier magnetic tunnel junctions

by

Bryan Kent Oliver

A dissertation submitted to the graduate faculty

in partial fulfillment of the requirements of

DOCTOR OF PHILOSOPHY

Major: Electrical Engineering (Microelectronics)

Program of Study Committee:
Gary Tuttle, Major Professor
Vik Dalal
Art Pohm
Joe Shinar
John Snyder

Iowa State University

Ames, Iowa

2003

UMI Number: 3105097

UMI®

UMI Microform 3105097

Copyright 2003 by ProQuest Information and Learning Company.

All rights reserved. This microform edition is protected against unauthorized copying under Title 17, United States Code.

ProQuest Information and Learning Company
300 North Zeeb Road
P.O. Box 1346
Ann Arbor, MI 48106-1346

Graduate College
Iowa State University

This is to certify that the doctoral dissertation of

Bryan Kent Oliver

has met the dissertation requirements of Iowa State University

Signature was redacted for privacy.

Major Professor

Signature was redacted for privacy.

For the Major Program

Table of Contents

General Introduction 1

Dielectric Breakdown in Magnetic Tunnel Junctions Having an Ultra-Thin Barrier 7

Tunneling Criteria and Breakdown for Low Resistive Magnetic Tunnel Junctions 25

Temperature and Bias Dependence of Dynamic Conductance – Low Resistive Magnetic Tunnel Junctions 40

Two Breakdown Mechanisms in Ultra-Thin Alumina Barrier Magnetic Tunnel Junctions 58

General Conclusions 87

Acknowledgments 89

General Introduction

Background

Around 1994, high tunnel magnetoresistance (TMR) was discovered for magnetic tunnel junctions (MTJs). TMR values of up to 50% have been widely reported, much higher than that of typical giant magnetoresistance (GMR) films. The tunnel junction resistance depends exponentially on the barrier thickness and is characterized by the resistance-area (RA) product. While early work reported large values of RA in the $G\Omega\mu m^2$ range, recent work has shown impressive TMR down below the 10 $\Omega\mu m^2$ range that is ideal for magnetic recording head applications. Low resistance is typically achieved by reducing the barrier thickness and oxidizing the barrier by exposing the metal to high-purity oxygen gas in a vacuum chamber.

The most critical layer in the MTJ stack is the barrier. The barrier for recording head applications is very thin, below 10 Å, and the RA product is dependent on the barrier thickness and degree of oxidation. In addition to being very smooth and uniform across the wafer, it is necessary to be free of pinholes. The presence of pinholes in the barrier layer of the MTJ are local shorts that can cause improper functioning of the device. Due to the nature of pinholes (or defects), their presence will typically increase as the barrier layer is decreased. The reduction of the MTJ barrier layer to achieve low RA products necessary for read head applications will require control of defects during growth in order to achieve properly functioning devices. Consequently, the development of low RA MTJs calls for detecting the presence of pinholes in the barrier.

To determine the presence of pinholes in the barrier, we need a solid set of criteria. The so-called Rowell criteria have typically been used in the discussion of tunneling phenomena. By satisfying as little as one of the three Rowell criteria, authors typically assume there are no pinholes present and that tunneling conduction dominates. However, as will be discussed in this Dissertation, these criteria by themselves are insufficient to judge the presence of pinholes in ultra-thin barrier MTJs. Without a solid set of criteria to judge the presence of pinholes, the electron conduction processes involved in the barrier cannot be accurately determined. Moreover, the presence of pinholes inherently affects such factors as the TMR response and the breakdown voltage of the barrier. Thus, the presence of pinholes can have strong implications on the parametric margins of the ultra-thin barrier MTJ for read sensor applications. What is needed is a simple criterion to use along side the Rowell criteria to judge the presence of pinholes.

Organization of the Dissertation

The organization of this Dissertation is as follows: Progressing from the standpoint of functioning ultra-thin barrier magnetic tunnel junctions, the breakdown mechanism of the barrier is studied and is observed to be related to the presence of pinholes in the barrier. Scrutinizing the MTJs using the Rowell criteria reveals that these criterion are insufficient in judging the presence of pinholes in ultra-thin barriers. However, with analysis of the breakdown mechanism, this deficiency is easily overcome. Recognizing that one type of breakdown is related to a pinhole-free barrier, the electron conduction processes in the barrier are revealed. Finally, intense studies using large ensembles of nominally identical MTJs

allow us to understand the root cause of the two observed breakdown mechanisms in ultra-thin barrier MTJs.

Work done for this Dissertation is comprised of four papers that have been published or at this time have been submitted for publication in the technical journals. A short synopsis of each of the four papers follows below.

1. Dielectric Breakdown in Magnetic Tunnel Junctions Having an Ultra-Thin Barrier

The presence of pinholes in the ultra-thin barrier is of major concern, as is the reliability of the barrier layer under stress. Two types of breakdown are observed in magnetic tunnel junctions having ultra-thin barriers: abrupt breakdown, which is determined by the thickness of the tunnel barrier, and gradual breakdown, which is related to defects in the barrier. Abrupt breakdown was observed in devices that consistently have TMR that is maximal before breaking, while gradual breakdown has TMR response that is lower. Breakdown results in irreversible damage to the MTJ resistance and TMR. Our studies suggest that after the breakdown event, a metallic pinhole is created, the size of which is dependent on the maximum current applied to the junction. Moreover, the current flowing through the short is shown to generate a strong circular magnetic field, curling the local magnetization in the free-layer around the pinhole, which in turn makes the free-layer reversal very sensitive to the location of the breakdown point in the junction area. The analysis of free-layer reversal shows the location of the metallic short is randomly distributed. The electrical properties after breakdown can be well described as an Ohmic resistor connected in parallel with a tunnel magnetoresistor.

2. Tunneling Criteria and Breakdown for Low Resistive Magnetic Tunnel Junctions

Criteria commonly used to identify tunneling behavior and judge the presence of pinholes in the barriers of MTJs, referred to as the Rowell Criteria, are scrutinized using the ultra-thin barrier MTJs measured at temperatures between 5K and 395K. These Rowell criteria are: (1) exponential thickness dependence of the resistance or conductance; (2) an insulating-like temperature dependence of the resistance or conductance; and (3) a non-linear characteristic of the current-voltage relation (I-V) that is fitted well to a rectangular model as described by Simmons (or differential conductance-voltage that is fitted well to a trapezoidal barrier as described in Brinkman's model). When these criteria are satisfied, it is typically believed that tunneling conduction dominates and that the barrier is pinhole-free. However, we show that these criteria in fact fail to detect the presence of pinholes in ultra-thin barrier MTJs. It is found that the study of breakdown mechanisms will dependably reveal the presence of pinholes in ultra-thin barriers. A first approximate model is presented, which describes the electrical properties of the MTJ as a tunnel magnetoresistor in parallel with a pinhole that behaves as an Ohmic short. It is proposed to include the study of breakdown mechanisms alongside the Rowell Criteria to judge the presence of pinholes in the ultra-thin barrier.

3. Temperature and Bias Dependence of Dynamic Conductance – Low Resistive Magnetic Tunnel Junctions

Ultra-thin barrier MTJs that have been determined to be pinhole-free are examined to understand the conduction process through the barrier. Effective barrier parameters can be estimated by fitting the dynamical conductance G(V) with the Brinkman-Dynes-Rowell model and fitting the temperature dependence of zero-bias conductance G(T) with the

Stratton model. However, a large discrepancy was discovered when comparing barrier parameters predicted by the two models. The inconsistency between the models is explained by the presence of an inelastic, spin-independent hopping conductance in addition to an elastic, spin-dependent tunnel conductance. The hopping conductance is strongly dependent on both temperature and voltage conductance, as described by the Glazman-Matveev theory of electron hopping. This additional hopping conductance helps explain the observed temperature dependence and bias dependence of magnetic tunnel junction conductance. Moreover, the strong influence of temperature on the hopping conductance reveals partly why the Rowell criteria are insufficient in judging pinhole presence in the ultra-thin barrier.

4. Two Breakdown Mechanisms in Ultra-Thin Alumina Barrier Magnetic Tunnel Junctions

The abrupt and gradual breakdown mechanisms that are observed in ultra-thin alumina barrier magnetic tunnel junctions are evaluated. It is desired to show that the breakdown mechanism is a clear and reliable indicator of the barrier quality. The two breakdown mechanisms manifest themselves differently when considering large ensembles of nominally identical devices under different stress conditions. The results suggest that the abrupt type of breakdown occurs because of the intrinsic breakdown of a well-formed oxide barrier that can be described by the E model of dielectric breakdown. An activation energy of intrinsic dielectric breakdown is found to be approximately 1.65-1.75 eV. The gradual breakdown is an extrinsic breakdown related to defects in the barrier rather than the failure of the oxide integrity. The characteristic of extrinsic breakdown suggests that a pre-existing pinhole in the barriers grows in area by means of dissipative (Joule) heating that occurs with an applied

power concentration of approximately 100 mW/μm^2 and/or an electric field in the range of 6.6-6.9 MV/cm across the pinhole circumference. Thus, the study of breakdown mechanisms can be used to determine the presence of pinholes (or defects) in the barrier.

Dielectric Breakdown in Magnetic Tunnel Junctions Having an Ultra-Thin Barrier

A paper published in the Journal of Applied Physics

Bryan Oliver, Qing He, Xuefei Tang, and J. Nowak

Seagate Technology LLC, 7801 Computer Avenue South, Bloomington, MN 55435

Abstract

Magnetic tunnel junctions have been fabricated by magnetron sputtering and patterned by deep ultraviolet photolithography. The tunnel magnetoresistance (TMR) was 15%-22% and resistance times area product (R×A) 7-22 $\Omega\mu m^2$ for junctions having 4.75-5.5 Å thick Al layer oxidized naturally. Two types of breakdown were observed: abrupt dielectric breakdown at effective field 10 MV/cm determined by the thickness of tunnel barrier, and a gradual breakdown related to defects in the tunnel barrier. After the breakdown a metallic pinhole is created, the size of which depends on the maximum current applied to the junction. The current flowing through the pinhole creates a strong circular magnetic field that curls local magnetization in the free layer around the pinhole. The subsequent free layer reversal is very sensitive to the pinhole location. The electric properties after breakdown can be well described by an Ohmic resistor and a tunnel magneto-resistor connected in parallel.

Introduction

In the last two years, great progress in lowering the product of resistance and area (RxA) has made possible a way to realize low-resistive tunneling reader for high-areal-

density recording.[1,2,3] Using Al layers thinner than 6Å oxidized in pure oxygen, R×A products lower than 10 $\Omega\mu m^2$ have been achieved.[1-4] However, it is observed that the tunnel magnetoresistance (TMR) drops almost linearly with R×A product. For example, for R×A = 5 $\Omega\mu m^2$, the TMR is about 15%, and for R×A = 1 $\Omega\mu m^2$, the TMR is only 3%. Dielectric breakdown has been examined in magnetic tunnel junctions with thicker barriers.[5,6,7] The breakdown voltage is much lower for the ultra-thin tunnel barrier.[8] In general, the lower breakdown voltage is related to a thinner tunnel barrier and/or the presence of pinholes.[9] In this article, we describe the effect of current stress on magnetic tunnel junctions with R×A in the range 7–22 $\Omega\mu m^2$. We will define two breakdown points corresponding to intrinsic and extrinsic failures. Intrinsic breakdown is related to the properties of ideal barriers and is determined by a critical electric field across the oxide layer. The extrinsic breakdown is defect-related (pinholes), and can be improved by reducing the roughness of the bottom electrode.

Experiment

Tunnel junctions were prepared on AlTiC wafers by DC magnetron sputtering in Ar atmosphere. The whole tunnel stack 50Ta/250PtMn/22CoFe/9Ru/22CoFe/x Al – ox/10CoFe/25NiFe/150Ta was grown in-situ on a bottom electrode. Four samples with Al thickness 4.75, 5, 5.25 and 5.5 Å were naturally oxidized. Sub-micron-size junctions were patterned using deep ultraviolet photolithography. Breakdown was examined using constant current mode for junctions having areas of about 0.2 μm^2. A typical current sweep begins at 0.2 mA with increments of 0.1 mA up to 25 mA. For each current step, the

magnetoresistance was measured in external magnetic range 2000 Oe which took about 3 seconds. The corresponding sweep rate was 3-4 mV/sec.

Results

Figure 1 shows a variation of R×A and TMR during constant current sweep of two junctions with 5-Å-thick barrier on the same wafer. For the junction with RxA = 9 $\Omega\mu m^2$ and 14% TMR (labeled by triangles) it is difficult to identify the breakdown point. Both resistance and TMR in Fig.1a and 1b vary gradually with applied current. The plot of R×A versus effective voltage in Fig.1c looks continuous; however, clear variation in the slope can be seen. Therefore, we conclude that this device deteriorates gradually, starting at an applied voltage of about 300mV. At any moment the gradual destruction can be stopped simply by lowering the current applied to the junction.

Identification of the breakdown point is much easier for the second junction with R×A = 14 $\Omega\mu m^2$ and TMR = 25% (squares). In this case the dielectric breakdown is abrupt. When the current reaches 13.6 mA, the junction resistance drops abruptly from about 10.4 to 6.4 $\Omega\mu m^2$ [Fig. 1(a)]. This device breaks down at more than two times larger voltage, about 665mV, than the previous one. Interestingly, during the breakdown event there is no abrupt change in TMR shown in Fig. 1(b) and 1(d). At the abrupt breakdown point the TMR = 5.3%, and as the current is further increased the junction damage gradually continues and TMR signal drops irreversibly. We distinguished two types of breakdown: a gradual breakdown at lower voltage and an abrupt breakdown at a much higher voltage. The gradual breakdown point can be precisely defined by looking at the plot of $\Delta V \equiv TMR \times V$ as a

function of voltage, shown in Figure 2. ΔV has a sharp maximum at V=280mV which defines the lower breakdown point.

We can now analyze in more detail what happens after the breakdown point. After the breakdown the current sweep was continued. During this final part of the current sweep (from breakdown to 25mA), the voltage across the junction is almost constant for both abrupt and gradual breakdowns (see Fig. 2). After the breakdown TMR varies linearly with effective R×A (see Fig. 3). Such a linear relation suggests that electron transport through broken tunnel junction can be described as a sum of two resistors connected in parallel. One resistor represents a pinhole created by the breakdown event and the other is the remainder of the tunnel junction. The pinhole material behaves like a conductor. Junctions with very large pinholes show a Joule heating effect – the resistance increases with applied current. Linear extrapolation to the zero TMR value gives the RxA product for metallic short – RxA_M ~ 0.8 $\Omega\mu m^2$. At this point the whole junction area is covered by metallic short and the tunnel junction is completely dead.

For the two examined devices, the slopes in Fig. 3 are different. This effect can be explained by the bias dependence of the TMR. The voltage across the high-resistive device after the breakdown is higher, 360mV, than the 320mV across the other one (see Fig. 2). As a result, the effective TMR for the first device is lower and the slope in Fig.3 is smaller. Similarly, the small variation of the slope for the low resistive junction can be attributed to TMR(V) dependence. TMR(280 mV) is slightly larger in comparison to TMR(320 mV) and as the result the slope in Fig.3 slightly varies.

So, a very simple model of magnetoresistive and normal resistors connected in parallel well describes the variation of TMR and R after the breakdown. Moreover, we can

estimate how large the metallic short is at the end of the current sweep. At that point both junctions show TMR = 2% and R×A = 2.8 $\Omega\mu m^2$. From these values we can estimate the area of metallic short to be 0.049μm^2. So, at the end of current sweep 23% of the junction area is occupied by metallic shorts. At the moment of abrupt breakdown of the high-resistive junction, a metallic short (pinhole) of a 0.017μm^2 area was created on what corresponds to 8% of the junction area.

It is interesting to compare the high- and low-resistive junctions shown in Fig.1-3. If we assume that the high-resistive junction with R×A = 14 $\Omega\mu m^2$ and TMR = 25% has no pinholes, we can then estimate that the second junction with 14% of TMR and R×A~ 9 $\Omega\mu m^2$ already has a pinhole or pinholes with a total area of 0.0076μm^2, corresponding to 3.6% of the total junction area. When the current is further increased, this pinhole does not grow up to the moment when current reaches 7.6 mA (V=280 mV). After that, the pinhole grows with current with the pinhole area roughly proportional to the applied current. The final size of the pinhole is determined by the maximum current applied to the junction. At any moment the growth can be stopped by simply lowering the applied current. This indicates that the growth process is thermally driven. The heat generated at the pinhole is so large that the electrode atoms can diffuse into barrier region and destroy it.

Hysteresis of the magnetoresistance was measured after each current step and we found very dramatic changes in the free-layer reversal at the breakdown point. Figure 4(a) shows the free-layer hysteresis before the breakdown. The magnetization of the pinned layer is pointing up and in zero external field and the direction of the free layer magnetization can be up or down, depending on the history. The hysteresis is centered at a field of H_1 = -6 Oe and the coercive field is about 22 Oe. The position and shape of the hysteresis is very

weakly dependent on applied bias current before the breakdown. Conversely, after the breakdown the free layer reversal is very sensitive to applied current. The upper part of Fig. 4(b) shows the free layer reversal for 10 mA current flowing from the bottom electrode to the top electrode. The whole free layer reversal is shifted towards negative field. The loop is centered at a field of -280 Oe and its coercive field is about 90 Oe. The bottom part of Fig. 4(b) shows the hysteresis loop for negative current direction. The whole hysteresis is shifted to the right and centered at 280 Oe. Reversing the current direction shifts the loop from –280 Oe to 280 Oe!

Such a shift can be simply explained by assuming that at breakdown a single metallic short is created somewhere inside the junction area. The metallic short will concentrate the current and a local circular magnetic field will be generated. With enough current, this local circular field is so strong that the free-layer magnetization curls around it and a magnetic vortex centered at the metallic short (pinhole) is created. From the shift of hysteresis we can judge the pinhole position. In our case, the pinhole must be located at the right side of junction – see the black spot in the schematic drawing of the junction area in Fig. 4(b). For positive current, a counterclockwise vortex is created. At the center of the free-layer, the magnetization points downwards and opposes the external magnetic field. Therefore, a very large negative external field is needed to complete the reversal. When the current is negative a clockwise vortex is created, the hysteresis loop is shifted to a positive field. From the loop shift we can estimate the position of the pinhole along a line perpendicular to the direction of the external field. Figure 5 shows the free-layer reversal for another junction after breakdown. The two loops correspond to bias currents –9.5 and 9.5 mA, respectfully. Both loops are very open, centered around H=0, and they show a wide narrowing in the center of

the loop. From this, we can conclude that a pinhole is located along a center vertical line parallel to the external magnetic field, as shown schematically in the inserts in Fig.5. The slope of the center part of the hysteresis loops in Fig. 5 contains information about pinhole location. When the pinhole is exactly in the center, the local circular magnetic field will be very strong around the junction circumference. Therefore, in low external fields, the vortex state is very stable and the central part of the loop shown in Fig. 5 is flat. If the pinhole is located along the central vertical line and far away from junction center, the average local circular field is much weaker, and as a result the slope of the hysteresis loop at H=0 is larger. Therefore, from the hysteresis loops in Fig. 5 we can conclude that the pinhole is located along the central vertical line, but we cannot tell if the pinhole is above or below the central vertical line. We notice that both loops in Fig.5 are slightly asymmetric. This simply indicates that in both cases the pinholes are located a little bit to the right side of the central vertical line. This illustrates how sensitive the loop shape is to the pinhole position. In reality, we may have few pinholes or even hundreds of them. However, there needs to be an asymmetry in the pinhole distribution to get such strong dependence of free layer reversal. Only detailed micromagnetic modeling can answer the question – how many pinholes are actually present in the examined devices.

The influence of current on hysteresis loop shape was examined for 64 other junctions. Figure 6 shows the distribution of H_l and the hysteresis slope at H=0 for applied bias current of 10 mA. H_l varies in a broad range of fields from –200 Oe to 280 Oe. Except for a few devices with low H_l, the majority of devices have very large both H_l and hysteresis slopes. This suggests that we have only one or a few pinholes in these cases. If the number

of pinholes is large, then the local magnetic fields from these compensate each other and we would expect to see no dependency of hysteresis shape on applied current.

Figure 7 shows a relation between average TMR and R×A for four samples with different Al thickness. All samples were naturally oxidized in the same conditions. For each Al thickness, 64 junctions were tested. The error bars in Fig. 7 indicate standard deviations. R×A product is very sensitive to the thickness of Al. Only 0.5 Å increase in thickness is causing 100% increase in RxA. In Al thickness range 5–5.5 Å TMR linearly drops, what reflects how total pinholes area varies with Al thickness. For the thinnest sample, 4.75 Å Al, there is a dramatic drop in the TMR which suggests that the pinhole area or the number of pinholes are much larger at this thickness. Figure 8 shows a variation of abrupt and gradual breakdown voltages with R×A product. Gradual breakdown voltages vary from 310 mV to 380 mV with Al thickness. The abrupt breakdown voltage for a 4.75-Å-thick Al layer is 570 mV, however, only two of 64 examined junctions were showing the abrupt type of breakdown. Similarly, only three of 64 junctions with 5 Å Al layer had showed the abrupt type of breakdown. For a 5.5-Å-thick barrier with R×A about 20 $\Omega\mu m^2$, 58% of the examined junction breaks abruptly. Notice that for each Al thickness there is a clear separation between lower and upper breakdown types. This suggests that the devices with upper breakdown point are essentially pinhole-free, and the dependence of abrupt breakdown voltage on barrier reflects an intrinsic property of ultra-thin barriers. Assuming that oxide thickness is 30% larger than Al thickness we can estimate that average electric field during the breakdown is about 9.2 MV/cm for 4.75 Å Al and 10.6 MV/cm for 5.5 Å of Al. These numbers are comparable to the breakdown fields of much thicker barriers prepared by plasma oxidation, about 10 MV/cm.[6] Our ultra-thin barriers break approximately at the same electric

field as twice as thick plasma oxidized barriers. In addition, this suggests that the devices with upper breakdown point are essentially pinhole free. However, a majority of devices break gradually and from this we conclude that it will be very challenging to make pinhole-free barriers with R×A below 10 $\Omega\mu m^2$. But a few samples show that it is possible to have ultra-thin barrier with breakdown voltage as high as 600mV.

In conclusion, tunnel junctions with ultra-thin tunnel barriers show abrupt (intrinsic) dielectric breakdown at 10 MV/cm. The gradual breakdown (extrinsic) at approximately 300mV is related to the presence of pinholes. The variation of TMR and R×A after the breakdown is consistent with a simple model of two parallel resistors – one an Ohmic resistor describing a metallic short and the other a magneto-resistor representing the remaining tunnel area. After typical intrinsic breakdown a metallic short is created and its area is of the order of a few percent of the junction area. The final size of the metallic short is determined by the maximum current applied to the junction. Current flowing through the metallic short generates a strong circular magnetic field which in turn creates a magnetic vortex state in the free layer. As a result, free layer reversal is very sensitive to the location of the breakdown point in the junction area. Analysis of free-layer reversal can be used to locate the metallic short.

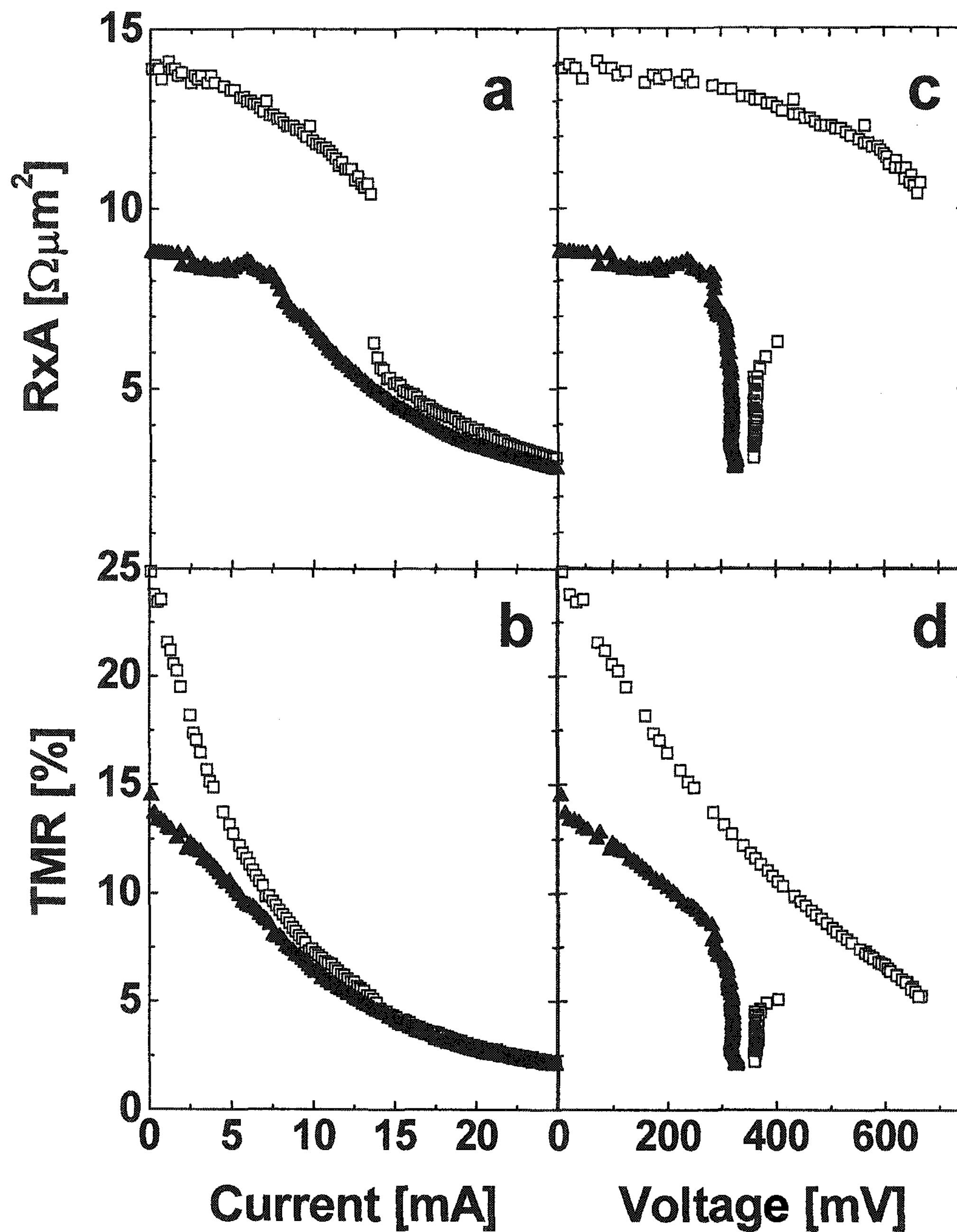

FIG. 1. TMR (a) and RxA (b) variation during constant current sweep for two junctions on the same wafer, one having RxA =9Ωμm^2 and TMR =14% (triangles), the other RxA =14Ωμm^2 and TMR =25%. Figures (c) and (d) show the same data on the voltage scale.

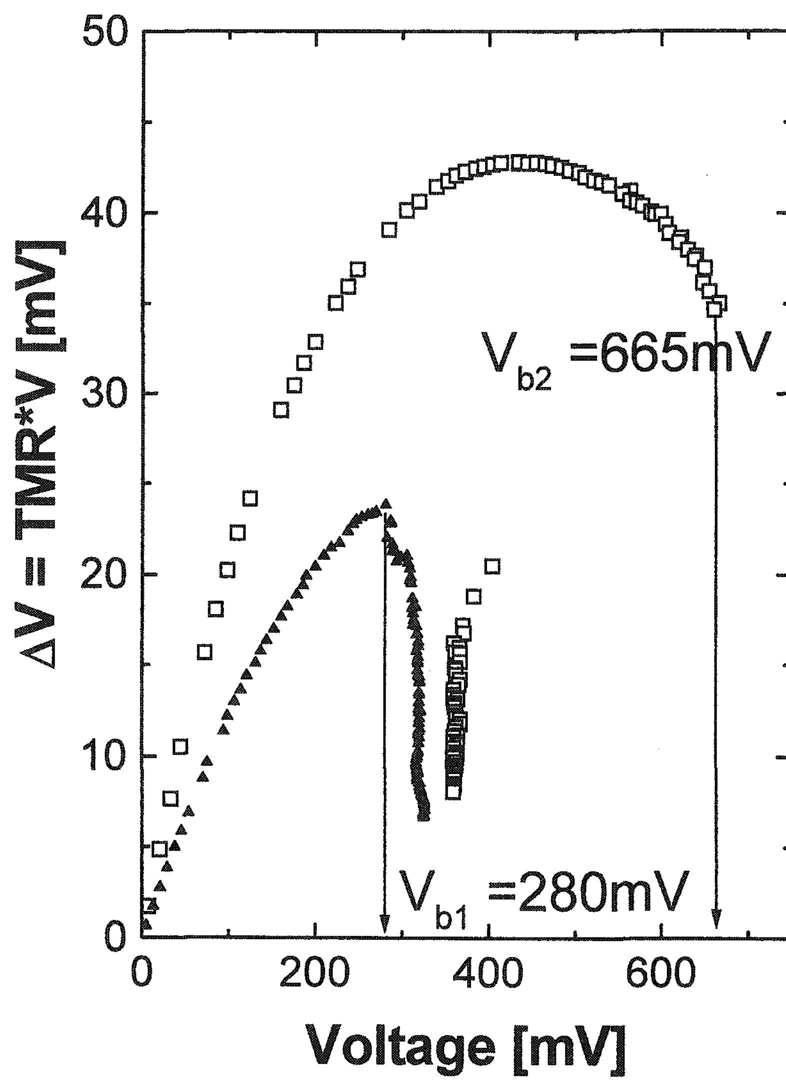

FIG. 2. TMR amplitude as the function of voltage during constant current sweep.

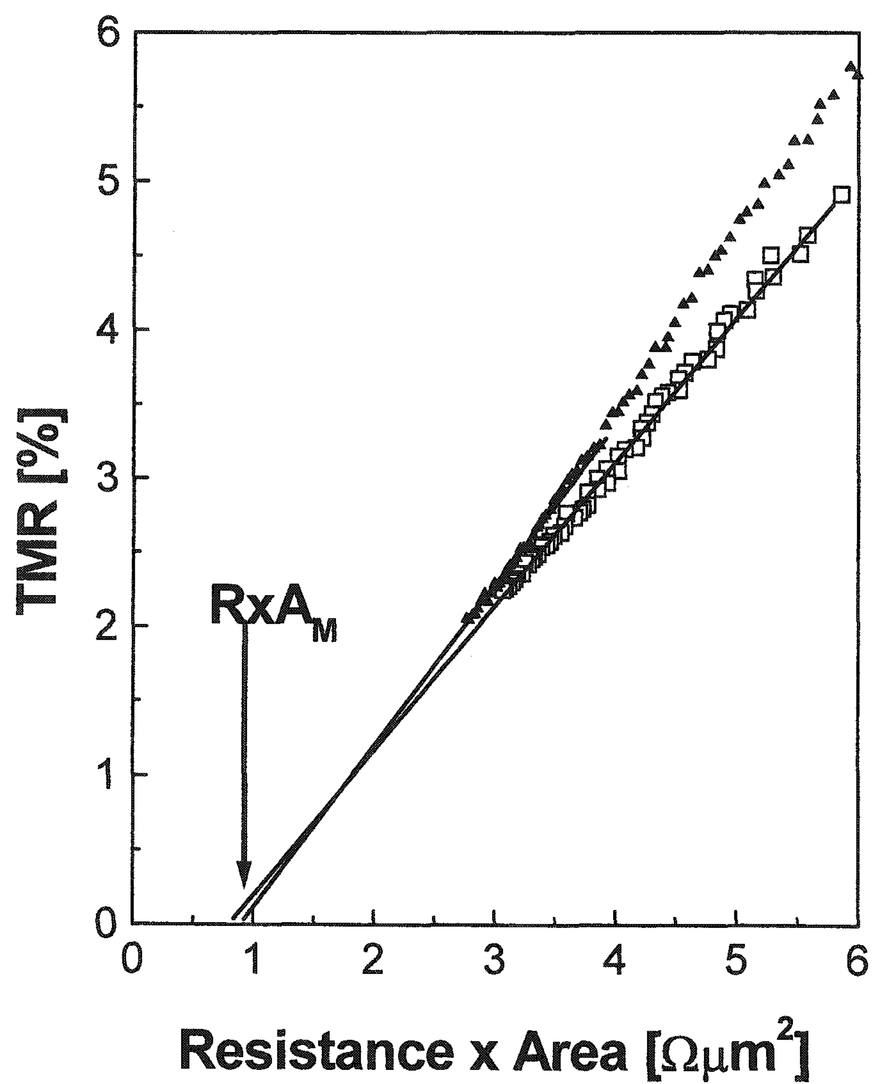

FIG. 3. After the breakdown TMR varies linearly with effective RxA.

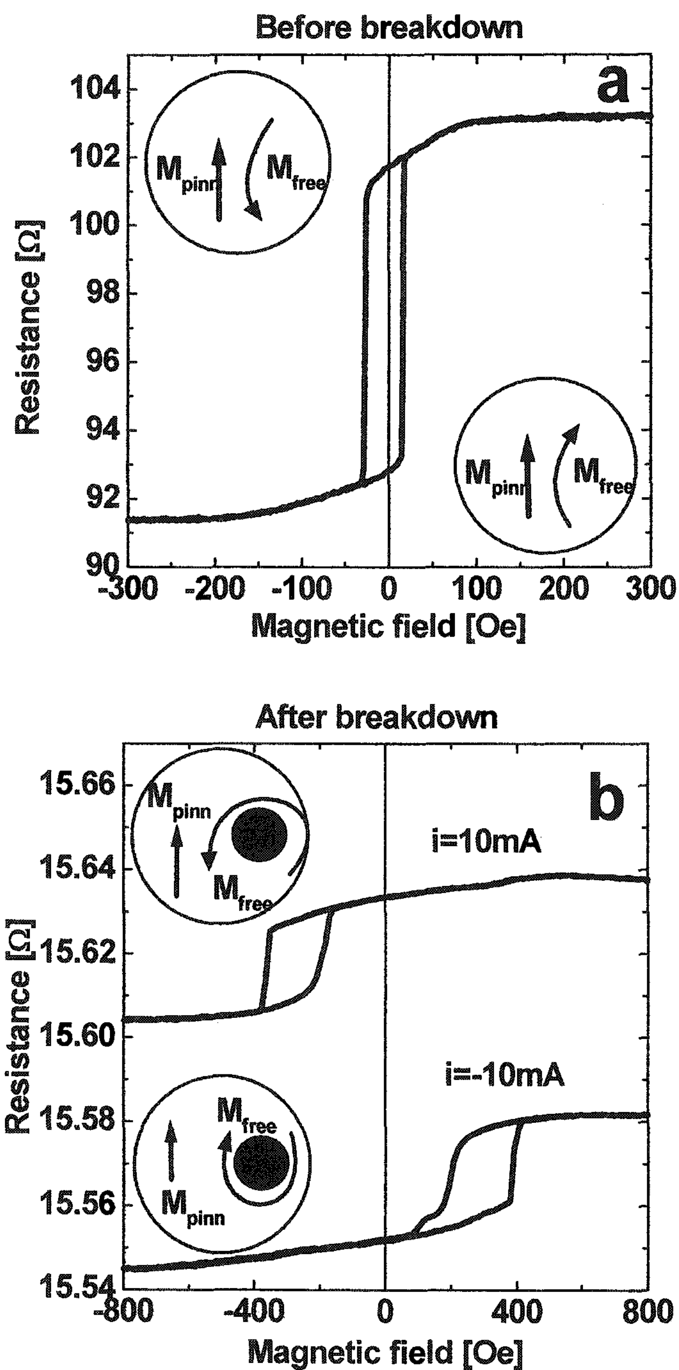

FIG. 4. Hysteresis of magnetoresistance before (a) and after (b) breakdown. A metallic short created at the breakdown point concentrates the current and a local circular magnetic field is generated. After the breakdown (b) the position of hysteresis loop strongly depends on current direction and amplitude.

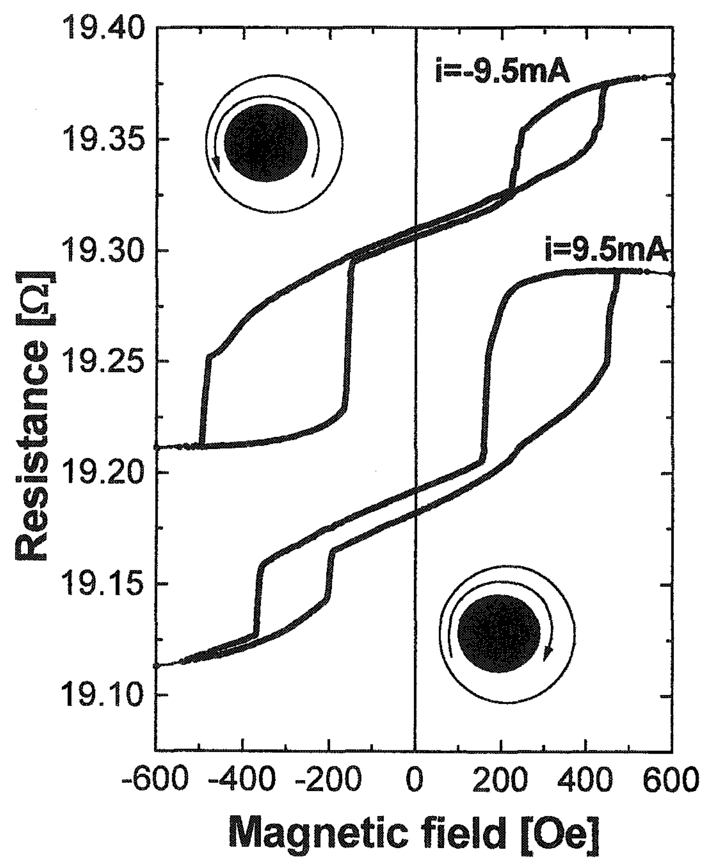

FIG. 5. Loop shape depends on current polarity and amplitude. The pinhole is located along a central vertical line parallel to external magnetic field.

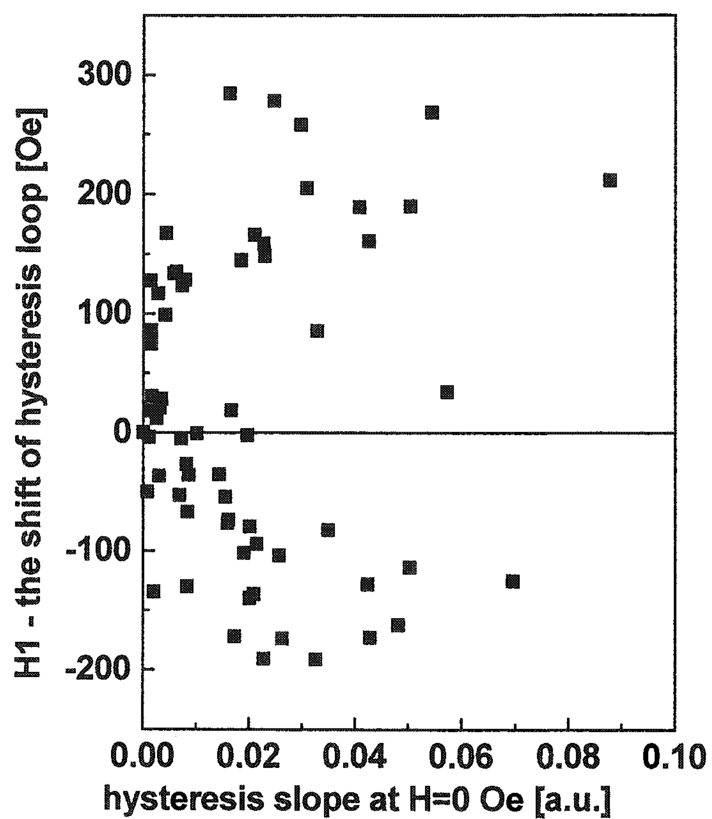

FIG. 6. Relation between H_1 and the hysteresis slope at H=0 for 64 examined junctions.

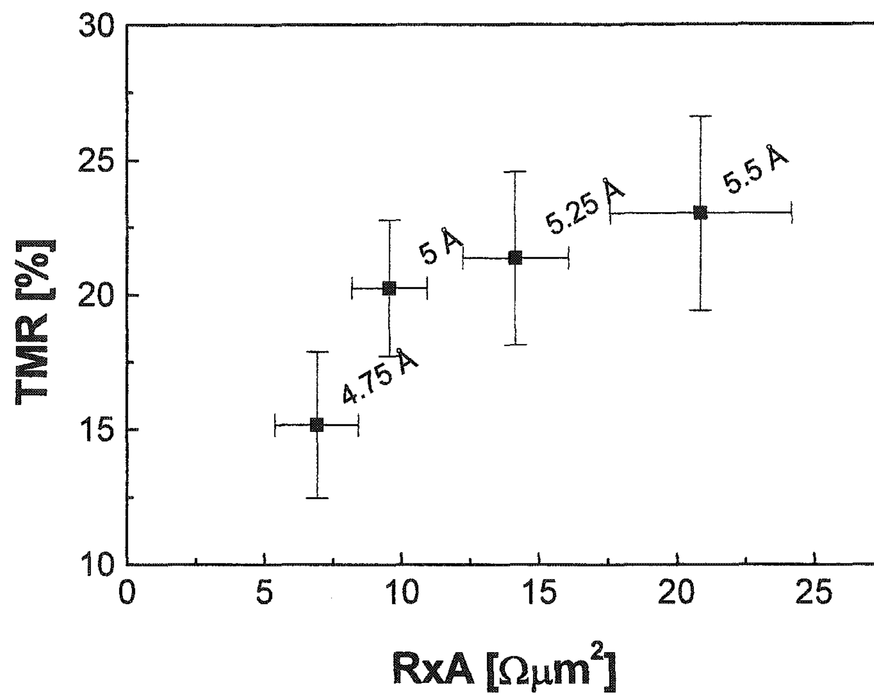

FIG. 7. Relation between average TMR and RxA for four samples with different Al thickness. All samples were naturally oxidized in same conditions. The error bars indicate standard deviations for 64 examined junctions.

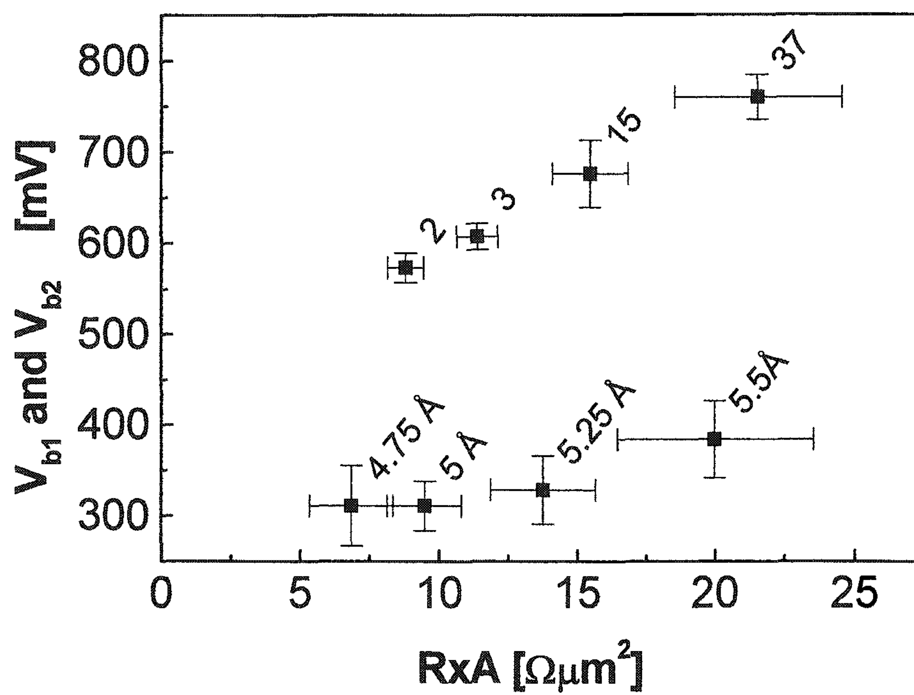

FIG. 8. Variation of abrupt and gradual breakdown voltages with RxA product. Error bars indicate standard deviations. Numbers of junctions breaking abruptly and Al thickness are also shown.

References

[1] J.J. Sun, K. Shimazawa, N. Kasahara, K. Sato, T. Kagami, S. Saruki, S. Araki and M. Matsuzaki, J. Appl. Phys. 89, 6653, (2001)

[2] J.R. Childress, M.M. Schwickert, R.E. Fontana, M.K. Ho, P.M. Rice and B.A. Gurney, J. Appl. Phys., 89, 7353, (2001)

[3] H. Boeve, J. De Boeck, G. Borghs, J. Appl. Phys., 89, 482, (2001)

[4] J.Fujikata, T. Ishi, S. Mori, K. Matsuda, K. Mori, H. Yokota, K. Hayashi, M. Nakada, A. Kamijo and K. Ohashi, J. Appl. Phys. 89, 7558, (2001)

[5] W. Oepts, H. J. Verhagen, R. Coehoorn, and W. J. de Jonge, J. Appl. Phys., 86, 3863, (1999)

[6] J. Schmalhorst, H. Bruckl, M. Justus, A. Thomas, G. Reiss, M. Vieth, G. Gieres and J. Wecker, J. Appl. Phys., 89, 586, (2001)

[7] K. Shimazawa, N. Kasahara, J. J. Sun, S. Araki, H. Morita and M. Matsuzaki, J. Appl. Phys. 87, 5194, (2000)

[8] D. Rao, K. Sin, M. Gibbons, S. Fulda, M. Mao, C. Chien, and H. C. Tong, J. Appl. Phys., 89, 7362, (2001)

[9] W. H. Rippard, A. C. Perrella and R. A. Buhrman, J. Appl. Phys. 89, 6642, (2001),
T. Dimopoulos, V. Da Costa, C. Tiusan, K. Ounadjela and H.A.M. van Berg, J. Appl. Phys., 89, 7371, (2001)

Tunneling Criteria and Breakdown for Low Resistive Magnetic Tunnel Junctions

A paper published in the Journal of Applied Physics

Bryan Oliver, Qing He, Xuefei Tang, and Janusz Nowak

Seagate Technology LLC, 7801 Computer Avenue South, Bloomington, MN 55435

Abstract

The tunneling criteria are evaluated using magnetic tunnel junctions having ultra-thin alumina barrier with and without pinholes. It is shown that the tunneling criteria formulated by Rowell [J. Appl. Phys. 42, 1915 (1970)] clearly do not rule out the presence of pinholes in an ultra-thin insulating barrier. In particular, the third criterion, a downward temperature dependence of resistance, cannot be used to decisively rule out the presence of pinholes. Examination of the breakdown mechanism will reveal the true nature of the barrier quality, and thus should be applied alongside the tunnel criteria to identify tunneling and the presence of pinholes.

Introduction

Interest in magnetic tunnel junctions (MTJs) is very strong, as the high, room temperature tunnel magneto-resistance (TMR) gives an advantage over existing giant magneto-resistance (GMR) devices.[1] For read head sensor applications, the reading data rate is increased and the head noise is reduced by using thinner and thinner barriers[2]. This requires the barrier thickness to be less than 10Å, prompting the question of how to rule out the presence of pinholes in the barrier. Pinholes are conductive shorts through the insulating

barrier and such defects can cause a dramatic reduction of the tunnel magnetoresistance by shunting the spin-dependent current with a spin-independent one[3]. Thus, a dependable set of guidelines is needed to test for the presence of pinholes and whether or not conduction is dominated by tunneling.

In magnetic tunnel junction structures, there are three Rowell criteria[4] that can be applied. First, the conduction should have an exponential barrier thickness dependence, such that $R(t) \sim \exp(t_{barrier}/t_o)$ where t_o is the Wentzel-Kramers-Brillouin decay length. Second, and the most prevalent in the literature for MTJ, the conduction should have a parabolic voltage dependence which should be well fitted to theoretical models of Brinkman-Dynes-Rowell[5] (BDR) or Simmons[6]. Finally, the conduction should have an insulating-like temperature dependence; i.e., the resistance will weakly decrease with temperature. As described in Akerman et al., the first two criteria – the thickness dependence and the voltage dependence of the conductance – are necessary, but not sufficient or reliable in ruling out the presence of pinholes in the barrier.[7,8] Their work evaluated Rowell criteria for magnetic tunnel junctions having RA of order of few kiloohms$\times\mu m^2$. The third criterion of the temperature dependence of the conduction clearly points out to the presence of the pinhole for high resistive MTJs [see Fig. 1(b) in Ref. 8]. In this paper we will show all three Rowell criteria for ultra-thin alumina barrier having RA of order of few tens of ohms$\times\mu m^2$ are inconclusive. As in Akerman et al.,[7,8] we intentionally created a short in the ultra thin alumina barrier, but contrary to their results we found tunneling like R(T) dependence for intentionally shorted device. Thus, additional tests are needed to judge pinhole presence in ultra-thin barriers.

MTJs are very sensitive to breakdown due to the thin insulating barrier. It is well known that after the breakdown, a conductive ohmic short is created in the oxide which causes device malfunction and reduction of the TMR effect.[3] What is not so clearly known is whether an intrinsic or extrinsic failure is causing the breakdown. Intrinsic breakdown is related to the voltage stress-induced degradation of a well-formed oxide, whereas extrinsic breakdown derives from process defects related to the deposition of the aluminum precursor layer and un-oxidized metal. We have recently demonstrated that the signature of intrinsic breakdown is an *abrupt* change in resistance at the breaking point, while a *gradual* change in resistance at the breaking point will be seen in devices failing extrinsically.[9] We have also shown that the effective voltage stays constant at around 300 mV during the growth of pinhole. This makes breakdown reliability studies an excellent tool for identifying either conduction by tunneling through an insulator or by ohmic transport in metal shorts.

We have examined magnetic tunnel junctions with ultra-thin insulating barriers thickness of 4.75-5.5Å and evaluated the results using the Rowell criteria. The devices inspected for each thickness are separated by virtue of the breakdown curve into those with and without pinholes. Our results suggest simple examination of the electrical breakdown mechanism will clearly and reliably identify the presence of pinholes, thus demonstrating the conduction process. Therefore, analysis of the breakdown mechanism should be used along with the Rowell criteria to more completely judge the barrier quality and test whether or not tunneling dominates the conduction in ultra-thin barrier MTJs. Unfortunately breakdown is a destructive test so we can evaluate the pinhole presence only statistically.

Experiment

The examined tunnel stacks have alumina barriers of four thicknesses (4.75, 5, 5.25, and 5.5 Å) with the structure 50Ta/250PtMn/22CoFe/9Ru/22CoFe/x Al–ox/10CoFe /25NiFe/150Ta grown in-situ on a bottom electrode. The substrate was an AlTiC wafer. Metal layers were deposited using DC magnetron sputtering in Ar atmosphere and the alumina barrier was formed by the natural oxidation of the aluminum layer. DUV lithography was used to pattern sub-micron size devices. We have not determined the actual thickness of the alumina layer, but differentiate between the barrier thickness by the deposited thickness of aluminum metal.

The current-voltage (I-V) curves were measured using four-point contacts and a constant current source from 5 to 400 K in a cryogenic tool manufactured by Quantum Design. G-V curves were obtained by numerically differentiating the I-V data. Both parallel and anti-parallel configurations were measured at ±500 Oe. Typical breakdown characteristics and breakdown voltages were known for these by examining large groups of devices[10], and as such, the voltage bias was kept well below the breakdown point in these experiments.

For the breakdown experiment, the devices were biased in a single voltage-ramp test using a constant current source. A typical sweep began at 10mV with 150 steps. Transfer curves were measured at each step in an external magnetic field of 1000 Oe. Before the breakdown test, TMR versus. RA was measured biasing the junction at 20mV using constant voltage source. 20mV was chosen because it is near the peak TMR response.

Results and Discussion

Two breakdown mechanisms observed in ultra-thin barriers of magnetic tunnel junctions were identified recently by us.[9] This can be seen in Fig. 1. Intrinsic failure due to voltage stress-induced degradation of an insulator is characterized by an abrupt decrease in resistance at the breaking point. Extrinsic failure of an insulator is due to process-related defects from limitations in deposition technology and the presence of ohmic shorts; its signature is a gradual decrease in resistance at the breaking point. After a breakdown event, a conductive pinhole is created that shunts the current. For a well-formed oxide, this means the bonds between the aluminum and oxygen are ripped apart and an ohmic channel is created, whereas a barrier with pinholes already has an ohmic channel which grows in size as the current sweep continues. After intrinsic breakdown effective voltage stays in the range 350mV- 410mV (Fig.1). It is noteworthy that after a device with a well-formed oxide fails intrinsically, each subsequent breakdown will be extrinsic due to growth of the pinhole created. Because of this distinction we can now separate devices into two classes of breakdown — devices that exhibit intrinsic breakdown or devices that exhibit extrinsic breakdown.

Evaluation of the first Rowell criterion shows roughly an exponentially dependent resistance on the barrier thickness (Fig. 2). Sixty four junctions were measured for each thickness and separated according to their respective breakdown characteristics. Separating the devices into breakdown classifications shows us that the resistance-area products expected for devices with a well-formed oxide are not distinct from those devices that suffer breakdown due to a pinhole in the barrier. Thus, the first Rowell criterion cannot help us in identifying pinhole presence.

Let us now look at the second Rowell criterion using the G(V) characteristics of a typical device 5.5Å Al barrier oxidized naturally (Fig.3). Knowing beforehand the typical breakdown voltages for devices showing similar RA and TMR, an I-V sweep is done below the breaking point and converted into a G-V sweep. This sweep is done in both parallel and anti-parallel configurations at ±500 Oe. Both measurements show similar G(V) trend and have a sharp cusp around zero-bias when at a liquid helium temperature of 5K. This zero-bias anomaly is ignored in modeling with the BDR model, and as such, we match the model to the curve on the wings typically at bias greater than ±200 mV. In the parallel configuration we find an effective thickness and barrier height of 5.48 Å and 1.49 eV respectively at 5K before intrinsic breakdown using the BDR model. After that, I-V curves were re-measured in a temperature range of 5K-395K. The device was then broken down by ramping the voltage and intrinsic breakdown was observed at 760 mV. After this breakdown, at 5K the barrier was 5.31 Å wide and 1.27 eV tall. The results before and after intrinsic breakdown are reasonable and typical for naturally oxidized ultra-thin alumina barriers and except for an increase in conduction level, the curves aren't significantly different. It is noteworthy the similarity between the two sets of data, considering we know that the G(V) shown in Fig. 3b has a large pinhole created intentionally. Thus, also the second Rowell criterion cannot clearly identify pinholes in the barrier.

We turn now to the third criterion, the temperature dependence of the conductance. Let us look at the 5.5Å Al thickness barrier that exhibits intrinsic failure at its breaking point and shows 45.0 Ohms and 24.5% TMR at 305 K. This sample would have typically more than 700 mV intrinsic breakdown voltage, so its I-V temperature dependence was measured in sweeps done in the range of ±600mV at each temperature. Examining the temperature

dependence of the normalized resistance before breakdown in Fig. 4 (circles) shows a weak, insulating-like curve, which is expected. After this test was done, the device was intentionally broken down, thus creating a pinhole. The resultant resistance was approximately half its initial resistance, 23.5 Ohms and TMR of 11.9% was observed. At this state the temperature dependence was re-examined with bias voltage kept below 300mV to avoid further growth of the existing pinhole. Seen in Fig. 4 (squares), after the first breakdown the normalized resistance exhibits weaker temperature dependence! So someone not knowing the device has a pinhole may naively conclude (looking at solid squares shown in figure 4) that a barrier is taller and/or wider than the initial barrier. The downward trend of the curve tells us that tunneling still dominates, but, at this point, it is clear the third Rowell criterion can completely mislead us by falsely indicating the barrier is better. Finally, the pinhole was grown further such that now the device is 11.2 Ohms with 4.8% TMR. The temperature dependence of this state was measured with the bias voltage again kept below 300mV and we found metal-like temperature dependence. Seen in Fig. 4 (triangles), the pinhole is now so large that ohmic-like conduction dominates the transport. It is remarkable that manipulation of the current compliance can create such a pinhole that the R(T) will be temperature independent.

The obtained results are consistent with the following models. A magnetic tunnel junction with a pinhole in the barrier can be modeled as a tunnel magneto-resistor in parallel with an ohmic resistor and its effective RA product can be described as

$$RA_{EFF}(x) = \frac{A}{\left(\frac{A-x}{RA_{INTRINSIC}}\right)+\left(\frac{x}{RA_{SHORT}}\right)} \qquad \text{Eq. 1}$$

where $RA_{INTRINSIC}$ is the RA product before breakdown (12.7 $\Omega*\mu m^2$), A is the total area of the device (0.28 μm^2), RA_{SHORT} is the RA product when TMR goes to zero (0.8 $\Omega*\mu m^2$) [9,10], and x is the area of the pinhole.[11] As for the TMR, when pinholes are present there will be competition between the tunnel current going through the undamaged part of the junction and the spin-independent current shunted through the pinhole. The effective TMR simply tracks the effective RA, which can be described as

$$TMR_{EFF}(x) = TMR_{INTRINSIC}\left(\frac{RA(x) - RA_{SHORT}}{RA_{INTRINSIC} - RA_{SHORT}}\right) \qquad \text{Eq. 2}$$

where $TMR_{INTRINSIC}$ is the TMR of the device before breakdown. Our results successfully follow these models as demonstrated in Fig. 5. Eq. 1 reveals the measured temperature dependence of the resistance will begin to show a *metal-like* dependence roughly when the pinhole area is beyond a threshold of

$$x > \frac{A \times RA_{SHORT}}{RA_{INTRINSIC} + RA_{SHORT}} \qquad \text{Eq. 3}$$

Eq. 3 is simply obtained by setting the denominator of Eq. 1 equal to zero, subtracting the two components from one another, then solving for x. For our low resistance MTJ, $RA_{INTRINSIC}$ is about one magnitude larger than RA_{SHORT}, and as such only a large pinhole occupying greater than ~20% of the total junction area can change the trend of R(T) curve from tunneling-like to metallic-like. Thus, it is not possible to identify even large pinhole's presence judging on a downward trend of temperature dependence of the resistance. Consequently, the third Rowell criterion is not sensitive to the presence of pinholes in MTJ having ultra-thin insulating barrier. The situation is different for a typical MTJ used in MRAM applications, which has a barrier thickness and a barrier height that is larger and as

such its $RA_{INTRINSIC}$ will be several magnitudes larger than RA_{SHORT}. Thus, any conductive short will quickly overcome the tunnel conduction and so the third Rowell criterion works well for high resistive MTJ to identify tunneling.[7, 8] For a low resistive MTJ, all three Rowell criteria can be fulfilled, yet they are not sufficient to prove tunneling dominates the transport. Only by examination of the breakdown mechanism are we able to determine the true barrier quality and identify the presence of a pinhole.

Conclusion

We have demonstrated that all three Rowell criteria are insensitive to the presence of pinhole in ultra-thin alumina barriers. They are necessary but insufficient conditions for judging the quality of tunneling. Especially, the third Rowel criterion – a downward temperature dependence of resistance cannot be used to decisively rule out the presence of pinholes. We propose to include analysis of electrical breakdown to judge about the pinhole presence. Unfortunately, the breakdown test is a destructive one, so we can assess quality of ultra-thin barrier only in a statistical sense. Moreover, different barriers and electrode materials may have different extrinsic breakdown voltages so the mechanism of pinhole growth can be material dependent.

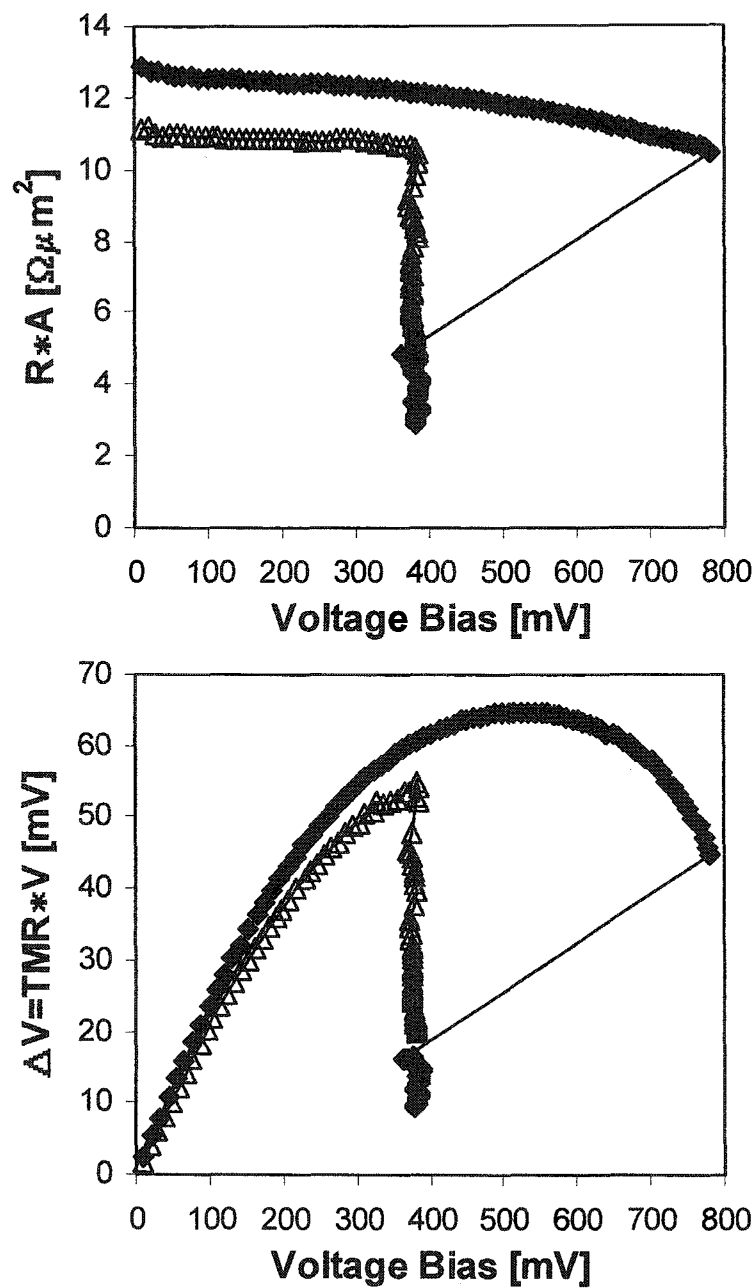

Figure 1. Variation of RA and ΔV during a constant current bias sweep. One junction breaks abruptly at 780mV and RA drops from 11 $\Omega\mu m^2$ to 5 $\Omega\mu m^2$ (solid diamonds). The second junction breaks gradually at voltage ~360mV (hollow triangles). In both cases after the breakdown bias sweep is continued, the pinhole grows and the effective voltage stays at the level 360mV.

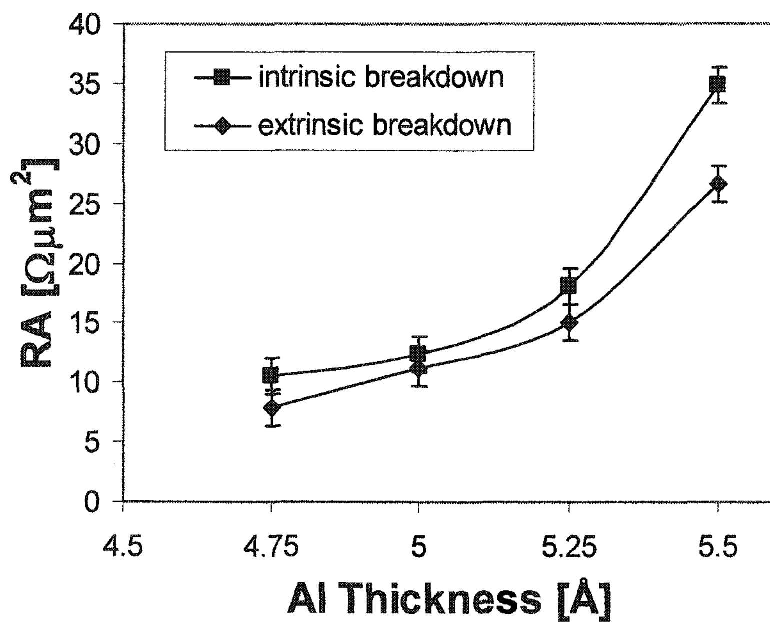

Figure 2. Average RA versus Al thickness for two groups of devices showing abrupt (intrinsic) and gradual (extrinsic) breakdown. For each Al thickness 64 devices were measured.

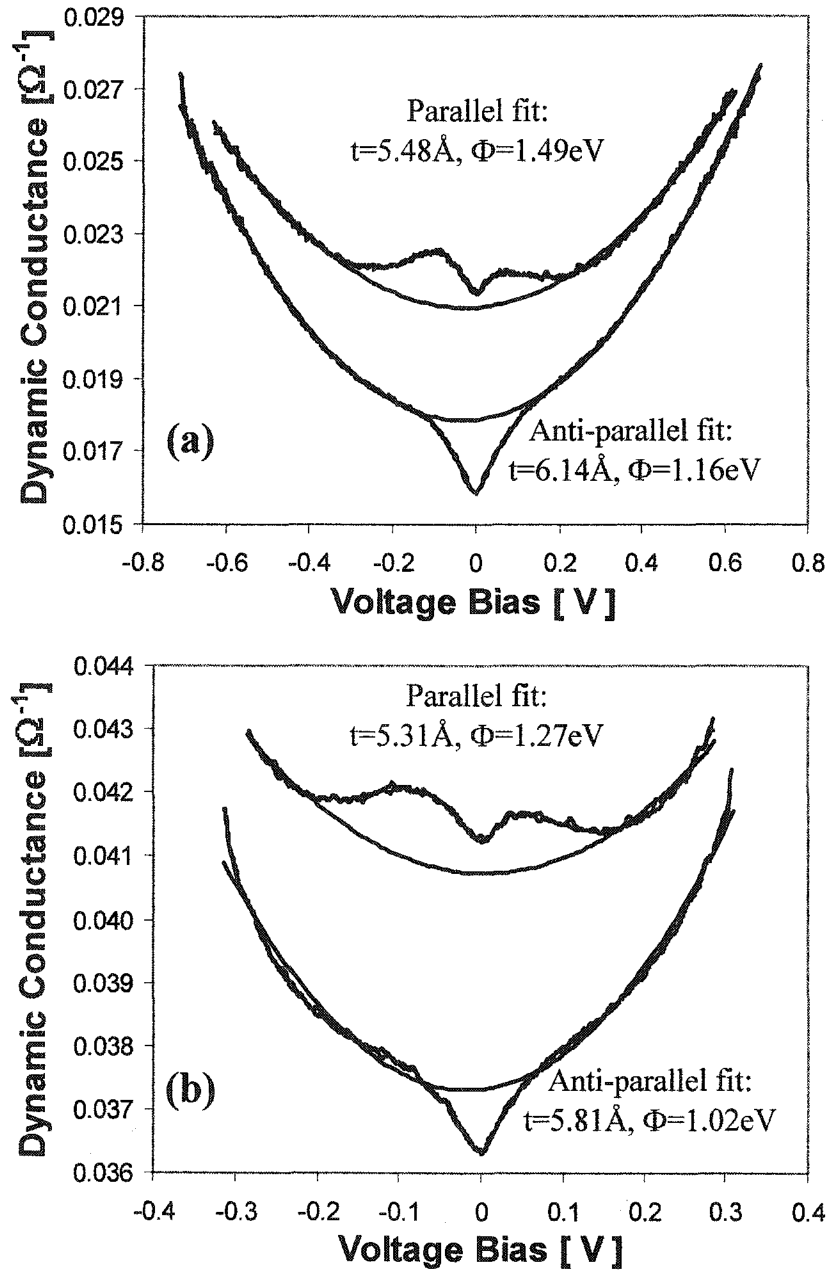

Figure 3. (a) G-V curves with fit to the BDR model for 5.5Å Al barrier at 5 K in parallel and anti-parallel configurations. (b) Same sample after intrinsic breakdown at 5 K.

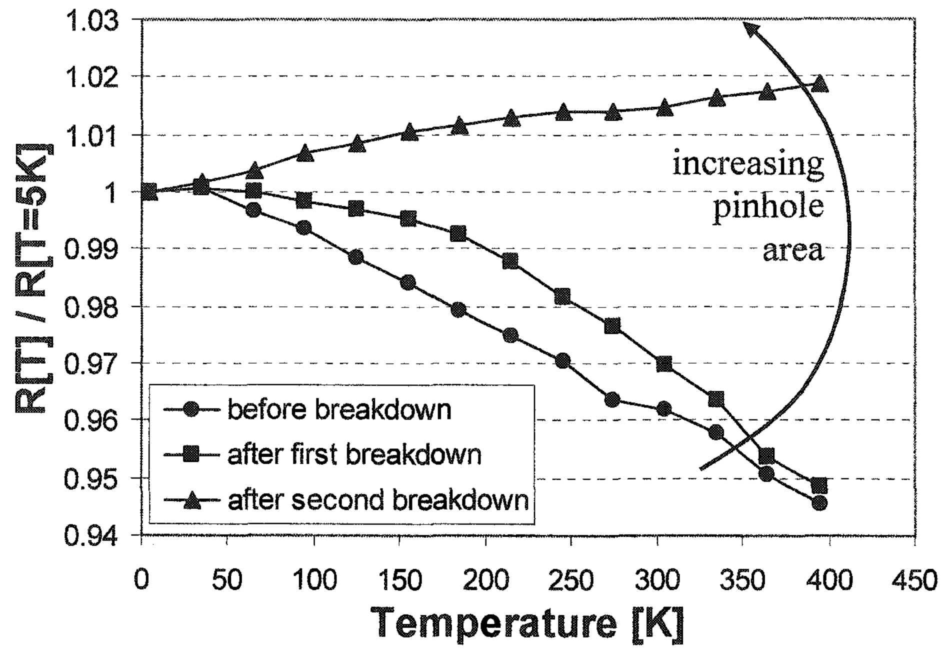

Figure 4. Normalized resistance versus temperature of one MTJ at three states. Before breakdown (circles), after the first breakdown (squares), and after the second breakdown (triangles).

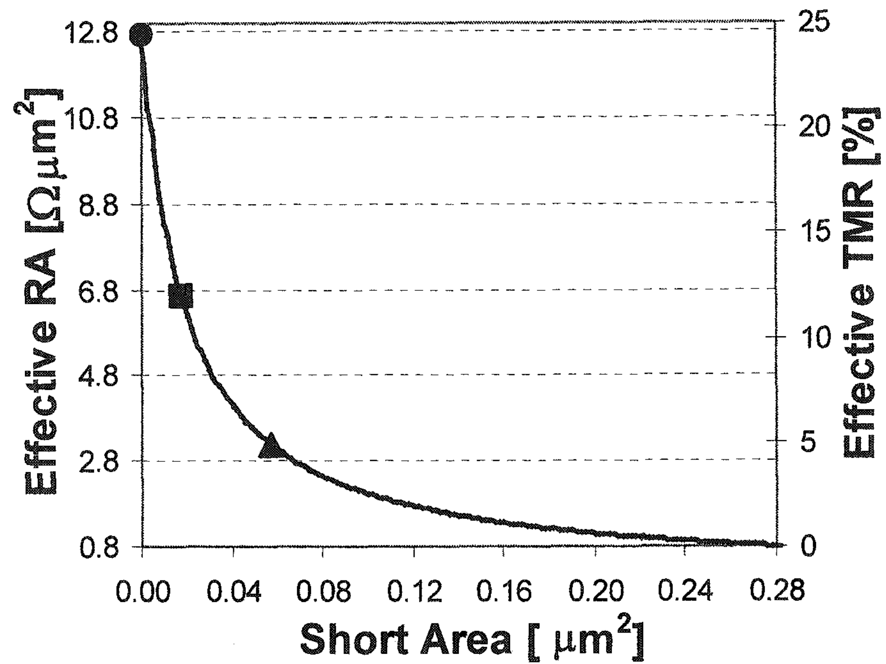

Figure 5. Effective RA and effective TMR versus short area. RA and TMR of the device before breakdown (circle), after intrinsic breakdown (square) and after further extrinsic breakdown (triangle). Metal-like temperature dependence can be observed when the short is ~20% of the device area (triangle).

References

[1] J. S. Moodera, Lisa R. Kinder, Terrilyn M. Wong, and R. Meservey, Phys. Rev. Lett 74, 3272 (1995).

[2] Hideyuki Kikuchi, Masashige Sato, and Kazuo Kobayashi, Fujitsu Sci. Tech. J. 37, 183 (2001).

[3] W. Oepts, H. J. Verhagen, W. J. M. de Jonge, and R. Coehoorn, Appl. Phys. Lett. 73, 2363 (1998).

[4] See e.g., Tunneling Phenomena in Solids, edited by Elias Burstein and Stig Lundqvist (Plenum, New York, 1969).

[5] W. F. Brinkman, R. C. Dynes, and J. M. Rowell, J. Appl. Phys. 41, 1915 (1970).

[6] John G. Simmons, J. Appl. Phys. 34, 1793 (1963).

[7] B. J. Jönsson-Åkerman, R. Escudero, C. Leighton, S. Kim, Ivan K. Schuller, and D. A. Rabson, Appl. Phys. Lett. 77, 1870 (2000).

[8] Johan J. Åkerman, J.M. Slaughter, Renu Whig Dave, Ivan K. Schuller, Appl. Phys. Lett. 79, 3104 (2001).

[9] Bryan Oliver, Qing He, Xuefei Tang, and J. Nowak, J. Appl. Phys. 91, 4348 (2002).

[10] Bryan Oliver, Qing He, Xuefei Tang, and Janusz Nowak, (in preparation).

[11] Estimation of the pinhole area critically depends on the value of RA_{SHORT} . This value was obtained from extrapolation of junction resistance having large pinhole. However, when the pinhole is very conductive we cannot neglect resistances of all the layers above and below it. Consequently, this estimation is actually the upper limit of the pinhole area.

Temperature and Bias Dependence of Dynamic Conductance – Low Resistive Magnetic Tunnel Junctions

A paper submitted to the Journal of Applied Physics

Bryan Oliver and Janusz Nowak

Seagate Technology LLC, 7801 Computer Avenue South, Bloomington, MN 55435

Abstract

I-V curves of magnetic tunnel junctions were measured in a temperature range of 5-305 K. Effective barrier parameters were estimated by fitting the dynamical conductance G(V) with the Brinkman-Dynes-Rowell model and fitting the temperature dependence of zero-bias conductance G(T) with the Stratton model. A large discrepancy was discovered when comparing barrier parameters predicted by the two models. The inconsistency between the models can be explained by the presence of an inelastic, spin-independent conductance that is strongly dependent on both temperature and voltage as described by Glazman-Matveev theory of electron hopping. This additional hopping conductance helps explain the observed temperature dependence and bias dependence of magnetic tunnel junction conductance.

Introduction

Barrier parameters can be extracted by fitting the dynamical conductance G(V) (dI/dV) to the Brinkman-Dynes-Rowell (BDR) model[1] or by fitting the temperature dependence of the zero-bias conductance G(T) to the Stratton model.[2,3] In determining the

barrier parameters from the BDR model, it is essential to make the proper fit to the data. At low temperatures tunnel junctions may have a zero-bias anomaly[4] – a narrow dip or a peak of G(V) around V = 0. Additionally, magnetic tunnel junctions have also low-bias anomalies – bumps in G(V) in the range of –200 to +200 mV. Usually, these are weakly dependent on temperature. As you can see from Figures 1 and 4, in the low bias range there is a dip in the conductance around V = 0 for both orientation of magnetization and a bump around –150 mV for the parallel orientation of magnetization. Notice that the dip in the conductance is a few times larger for the antiparallel orientation and it is strongly temperature dependent. The bump in conductance for parallel orientation is weakly dependent on temperature and can be identified even at 305 K. The details of low-bias anomalies and its origin are not addressed in this paper.

To minimize the impact of bias anomalies on fit quality, we propose to fit only the arms of the experimental G(V) curve to the model. We recommend fitting simultaneously both arms of G(V) to the BDR model. Typically we use a voltage ranges from –0.6 V to –0.2 V for the left G(V) arm and the range from +0.2 V to +0.6 V for the right G(V) arm. In the case of fitting I(V) to a model (Ref. 2), the bias anomalies are completely invisible on the I(V) curves. As a result, the quality of the I(V) fit is usually poor and the errors of the extracted barrier parameters are much larger. Moreover, for I(V) fits, any constant resistance term is included in the fit and impacts barrier parameters. These make fitting to the arms of dynamic G(V) a better choice, as it allows us to minimize the errors and to clearly identify the low-bias anomalies by comparing data with the fit in the low voltage range.

We extract barrier parameters with the BDR model using this technique and use the zero-bias conductance of this technique for G(T) to obtain barrier parameters with the

Stratton model. To be clear, the zero-bias conductance is the value taken not from the G(V) data curve, but from the trend line fit at V = 0. This allows us to be consistent in ignoring the low-bias anomalies for both parallel and anti-parallel magnetizations. The spin-independent conductance term we present later in this paper is thus extracted from dynamical G(V) curves for both parallel and anti-parallel magnetization orientations.

Experiment

The examined tunnel stacks have the structure 50Ta/250PtMn/22CoFe/9Ru/22CoFe/Al–ox/10CoFe /25NiFe/150Ta grown in-situ on a bottom electrode. The substrate was an AlTiC wafer. Metal layers were deposited using DC magnetron sputtering in Ar atmosphere and the alumina barrier was formed by the natural oxidation of the aluminum layer. DUV lithography was used to pattern sub-micron size devices.

The I-V curves were measured using four-point contacts and a constant current source from 5-305 K in a cryogenic tool manufactured by Quantum Design. G(V) curves were obtained by numerically differentiating the I-V data. Both parallel and anti-parallel configurations were measured at ±500 Oe. Typical breakdown characteristics and breakdown voltages were known for these junctions by examining large groups of devices[5], and as such, the voltage bias was kept well below the breakdown point in these experiments.

Results and Discussion

Figure 1 shows the dynamic conductance G(V) for parallel and anti-parallel magnetization of 5.0 Å Al naturally oxidized magnetic tunnel junction at T = 5 K. While both curves show a significant low-bias anomaly, the wings of the curves are parabolic. The

solid lines represent the trend fitting to the data. In the range of -0.2 to -0.6 V and +0.2 to +0.6 V, fitting to the Brinkman-Dynes-Rowell model[1] can be done. This model is given by

$$G(V) = G_0\left[1 - \left(\frac{A_0 \Delta\phi}{16\bar{\phi}^{3/2}}\right)(qV) + \left(\frac{9}{128}\frac{A_0^{\,2}}{\bar{\phi}}\right)(qV)^2\right] \quad \text{Eq. 1}$$

where

$$\Delta\phi = \phi_2 - \phi_1, \quad \text{Eq. 2}$$

$$A_O = \frac{4t\sqrt{2m}}{3\hbar} \quad \text{Eq. 3}$$

$$G_O = \left(\frac{q^2}{th^2}\right)\sqrt{2qm\phi}\exp\left(-\frac{t\sqrt{8mq\phi}}{\hbar}\right) \quad \text{Eq. 4}$$

The barrier thickness t is in Å and the barrier height ϕ is in Volts. From this model, we obtain t = 5.52 Å and ϕ_{AVE} = 1.14 eV for parallel magnetization and t = 6.22 Å and ϕ_{AVE} = 0.871 eV for antiparallel magnetization.

Shown in Figure 2 is the temperature dependence of the zero-bias resistance (which is the inverse of zero-bias conductance) for the same sample. According to Stratton model,[3,4] the zero-bias G(T) characteristic can be described as

$$G(T, V = 0) = \left.\frac{I/Area}{V}\right|_{V \to 0} = \frac{4mq^2\pi^2 k}{Ch^3}\exp(-B) \times \left[\frac{CT}{\sin(CT)}\right] \quad \text{Eq. 5}$$

where

$$C = \frac{\pi kt}{\hbar}\sqrt{\frac{2m}{q\phi}} \quad \text{Eq. 6}$$

$$B = \frac{t\sqrt{8mq\phi}}{\hbar} \quad \text{Eq. 7}$$

with barrier thickness t in Å and the barrier height ϕ in Volts. The solid line in the plot of Figure 2 shows a direct fit of the measurements to the Stratton model, from which we obtain t = 7.52 Å and ϕ_{AVE} = 0.471 eV for parallel magnetization and t = 8.28 Å and ϕ_{AVE} =0.383 eV for antiparallel magnetization. So, it is found the two models give very different barrier parameters!

It has been theorized that in magnetic tunnel junctions, in addition to the spin-polarized *elastic* tunneling conductance, there is also a spin-independent *inelastic* conductance that is strongly influenced by temperature.[6] For a device without pinholes, this conductance would be described by the following:

$$G(T,V) = G_{Elastic}(T,V) + G_{Inelastic}(T,V) \qquad \text{Eq. 8}$$

The inelastic conduction channel can be explained by the Glazman-Matveev (GM) theory[7] of electron hopping. In this theory, the conductance of the hopping channel exhibits a characteristic temperature dependence that follows a power law, $G_N^{Hop}(T) = \tau_N T^{\gamma}$. τ_N is a parameter that is proportional to the density and radius of the localized hopping states as well as the barrier thickness and γ is given by $\gamma(N) = N - [2/(N+1)]$. N is the number of hopping steps that an electron takes in passing through the barrier. It is important to note that $\gamma(N)$ is not continuous. In the case of second order hopping (N=2), $G_2^{Hop} \propto T^{1.33}$, whereas in the case of higher, third order hopping, $G_3^{Hop} \propto T^{2.5}$, and so forth. In the G-M theory, there also exists a similar characteristic voltage dependence of hopping conduction, $G_N^{Hop}(V) = \nu_N V^{\gamma}$, where ν_N is a parameter similar but not equal to τ_N. It should be noted that $G_N^{Hop}(T)$ and

$G_N^{Hop}(V)$ are applicable for eV << kT and eV >> kT, respectively, and valid as long as eV is smaller than the barrier height.

Temperature Dependence of the Dynamic Conductance

Let us proceed from the assumption for our sample there is present inelastic hopping conduction in addition to the elastic tunneling conduction. In this case, the barrier parameters obtained using the BDR model at low temperature of 5K would yield trustworthy results. This is because at low temperature, the hopping conductance would be minimal, and as such, the G(V) characteristic would be almost purely tunneling conduction. In contrast, the Stratton model, in which the barrier parameters are based on R-T characteristics over a wide range of T, would yield unreliable results because of the influence of the hopping conductance and its strong dependence on temperature in the measurement.

The influence of temperature on the hopping conductance can be evaluated by combining the BDR model barrier parameters obtained at T = 5 K within the Stratton model (Eq. 5). We have already ruled out the presence of pinholes.[5,8] With this correction, theory predicts a decrease in the resistance with temperature of only 0.79% decrease for parallel magnetization barrier parameters of t = 5.52 Å and ϕ_{AVE} = 1.14 eV and only a 1.3% decrease for anti-parallel alignment barrier parameters of t = 6.22 Å and ϕ_{AVE} = 0.871 eV. However, the experimental measurements show a much larger decrease in the temperature dependence of the zero-bias resistance: 3.6% and 4.7%, respectively, for parallel and anti-parallel alignment in the temperature range of 5-305 K. So, for our device there is a large discrepancy between theoretical prediction and experimental data.

We can explain the R(T) characteristic of Figure 2 by showing a fit to the data for the entire range of temperature 5-305 K with the form

$$G(T,V=0) = G_{T_Stratton}(T,V=0)\Big|_{\substack{BDR_parameters \\ T=5K}} + \tau_2 T^{1.33} \qquad \text{Eq. 9a}$$

or alternatively,

$$G(T,V) = \left[\frac{CT}{\sin(CT)}\right] \times G_{T_BDR}(T,V)\Big|_{\substack{BDR_parameters \\ T=5K}} + \tau_2 T^{1.33} \qquad \text{Eq. 9b}$$

Eq. 9a is Eq. 5 with an additional term to account for the onset of spin-independent hopping conductance processes. The Stratton model is evaluated using BDR parameters obtained at T = 5 K for parallel state and anti-parallel orientations. Alternatively, we could choose Eq. 9b evaluated at V = 0, in which the first term of Eq. 9a is replaced with the BDR model of Eq. 1 multiplied by the Stratton temperature correction factor. A good fit for the entire range of temperature (T ≥ 5 K) is obtained with second order (N=2) hopping conduction, which follows dependence of temperature $T^{1.33}$ with $\tau_2 = 2.3\times10^{-7}$. We stress that it is because of the presence of hopping conductance that the BDR and Stratton models give different barrier parameters. As such, it is possible to generate the solid trend line in Figure 2 in two ways: first, by direct fitting of the data, albeit erroneously, to the Stratton model of Eq. 5; second, by fitting using the BDR model barrier parameters with the addition of spin-independent hopping conductance as given in Eq. 9.

Voltage Dependence of the Dynamic Conductance

Shown in Figure 3 is the influence of the voltage bias on the dynamical conductance at several temperatures for both magnetization orientations. The solid line in each plot

represents the bias dependence trend fitting at T = 5 K but offset because the temperature dependence follows $T^{1.33}$. It was found that for T > 200 K, the experimental G(V) curves become steeper and steeper when compared to the fitted ones. Classical tunnel theory[2] suggests G(V) should only track the slight change in resistance with temperature. Furthermore, using a direct fit to the BDR model of Eq. 1, the effective barrier parameters change very little for T < 200 K; however, they show a strong dependence on temperature for T > 200 K. See Figure 4. By increasing the temperature T > 200 K, it appears as though the effective thickness increases and the effective barrier height decreases. Classical tunnel theory[2] also suggests the barrier parameters should not change with temperature. Once again, for our device there is a discrepancy between theoretical prediction and experimental data.

These results can be interpreted as the presence of an additional conductance channel that is influenced by the bias voltage but is separate from the temperature dependent hopping channel. At T= 5 K, the influence of the spin-independent hopping conductance on G(T) is minimal, so it is assumed the influence of voltage hopping conductance on G(V) is negligible. For T< 200 K, the effective barrier parameters change very little. This can be interpreted as negligible influence of voltage-dependent hopping conductance in this temperature range. Increasing temperature to T = 155 K, it the G(V) characteristic for either magnetization state is still well fit to similar trend at T = 5 K. Increasing the temperature further to T = 305 K, the majority of the data curve, even the low bias regime (for V < –0.2 and V > +0.2 V, which excludes the anomalies) does not follow the trend of the bias dependence at T = 5 K. However, by recognizing that the barrier parameters are constant with temperature, we can account for this influence by using Eq. 9b with the addition of a

term $\nu_N V^{1.33}$ that represents the onset of second order voltage dependent hopping processes. A good fit is obtained with $\nu_2 = 0.001$. The combined effect of high temperature and bias promotes the activation of a voltage dependent hopping conductance channel.[7] Note that for this sample, the change in barrier parameters is negligible for T < 200 K; however, the barrier parameters have a strong dependence on temperature for T > 200 K, which coincides with the onset of voltage-dependent hopping. Consequently, the presence of the spin-independent hopping conductance would account for the apparent temperature dependence of the BDR barrier parameters.

At around room temperature of T = 305 K, it is estimated that the zero bias spin-independent hopping conductance is of the order of 2.9% of the total conduction, whereas it is increased to around 4.3% at bias of 500 mV, which for this particular barrier is close to its breakdown voltage. Similar fits shown in Table 1 were obtained for naturally oxidized aluminum of thickness 5.25 and 5.5 Å and for 15 Å aluminum oxidized by glow discharge. For thick Al barrier, a best fit could not be obtained with second order hopping. Instead, it was necessary to add a third order temperature term above T= 125 K and third and fourth order voltage dependent terms. The theory clearly states that increasing temperature or bias voltage as well as increasing barrier thickness favors hopping along chains of increasing number of states (N>2).[7,9] Consequently, this thicker barrier at T = 305 K has 12.4% of the total as spin-independent hopping conduction. The amount of hopping conductance is a direct indicator of barrier quality. For good thick barriers at room temperature, 10%-25% of total conductance can originate from hopping. For our ultra thin barriers, only 3% of

conductance origins from hopping processes because for ultra thin barriers direct elastic tunneling is preferred.

It is interesting to note that 15 Å Al oxidized by glow-discharge gives a barrier height around 2.86 eV. This is typical for alumina in magnetic tunnel junctions. A much thinner barrier made from naturally oxidized aluminum yields a barrier height around 1.14 eV. Increasing the deposition thickness to 5.25 and 5.5 Å doesn't increase the thickness, but does increase the barrier height to 1.35 and 1.49 eV, respectively. This is probably because there are weak spots in the oxide where the barrier thickness can be less than its nominal thickness or the barrier is oxygen deficient. The current is concentrated on these weak spots because the current going through the oxide is exponentially dependent on the thickness and barrier height. It is difficult to tell if these weak spots behave as tunneling, hopping, or even ohmic conductors. Studies of electrical breakdown, which is a weakest-link type of analysis, show that the weak spots are the origins of the breakdown of the oxide. While it is believed in this study that all junctions had a good quality oxide barrier with only tunneling and hopping conduction, the ohmic current may not be insignificant.

Conclusion

We have demonstrated that there is a large discrepancy between barrier parameters estimated by direct fitting of dynamical conductance G(V) with the BDR model and direct fitting of the temperature dependence of the zero-bias conductance with the Stratton model. The inconsistency between these models can be explained by the presence of a spin-independent hopping conductance described by Glazman-Matveev theory in addition to the spin-polarized tunnel conductance. This additional hopping conductance explains the

temperature dependence and voltage dependence of magnetic tunnel junction conductance. For ultra thin barriers, hopping conductance is greatly reduced in comparison to thicker barriers used for MRAM.

The presence of an additional conduction channel consequently makes the Stratton model unreliable in determining barrier parameters because the data includes both elastic and inelastic conduction channels, whereas the fit would be made to a model based solely on pure elastic tunneling. Extracting barrier parameters from the BDR model at low temperature makes a much better choice because the influence of the inelastic conduction is minimal, especially at liquid helium temperatures. Therefore, it is believed the barrier parameters as given by the BDR model at low temperature are correct.

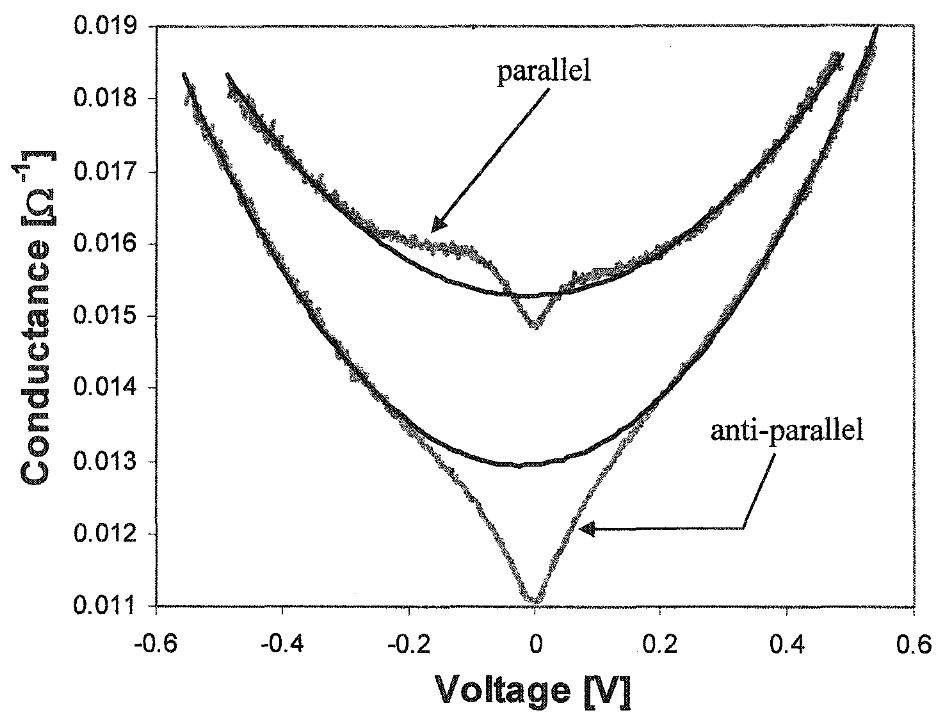

Figure 1. Parallel and anti-parallel dynamic conductance at T=5 K. Only conductance arms in the range of –0.2 to –0.6 V and +0.2 to +0.6 V were fit to the BDR model. The smooth solid lines represent the fits.

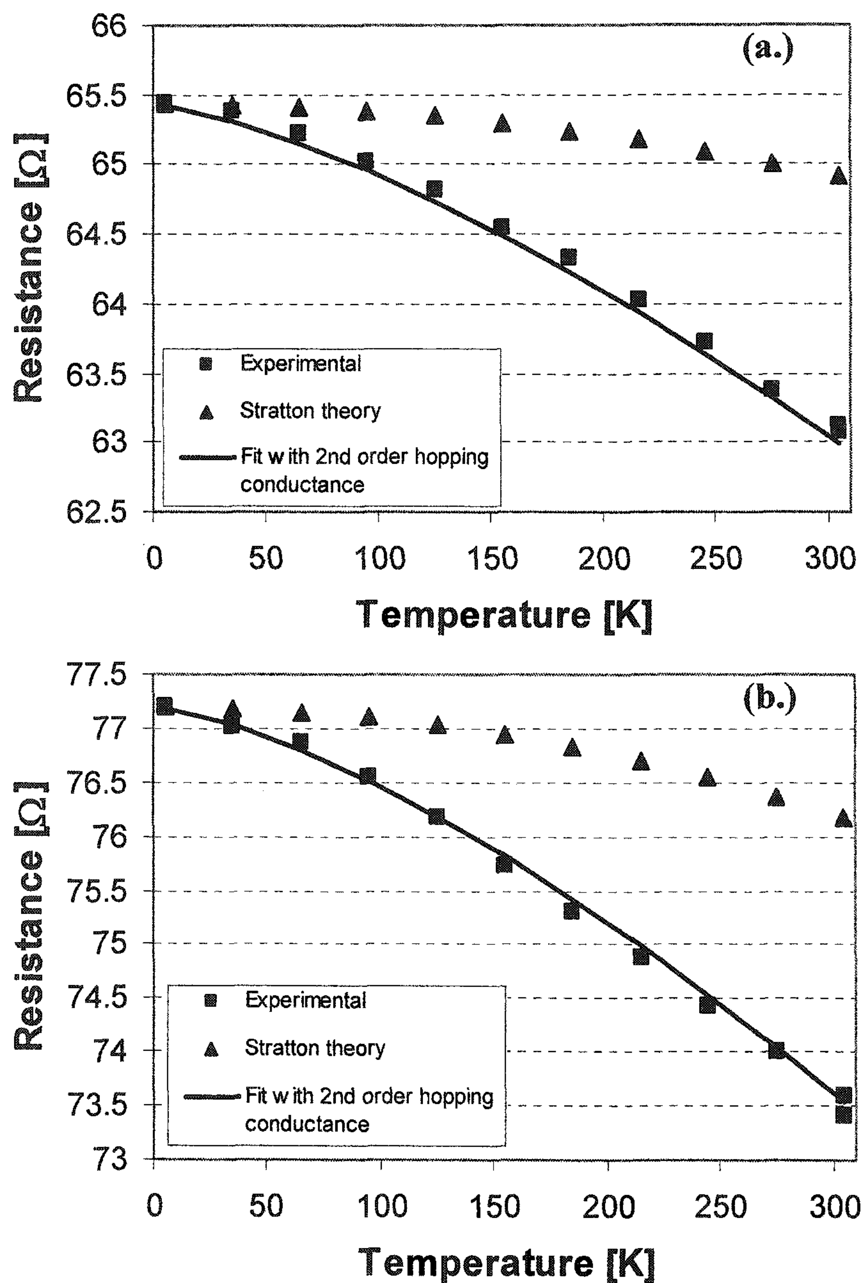

Figure 2. Temperature dependence of the zero-bias resistance (squares) for (a.) parallel and (b.) anti-parallel magnetization orientation. Stratton model predicts much weaker temperature dependence (triangles). The solid line can be obtained in two ways: a direct fit to the Stratton model or a fit using BDR barrier parameters with the addition of second order hopping conduction.

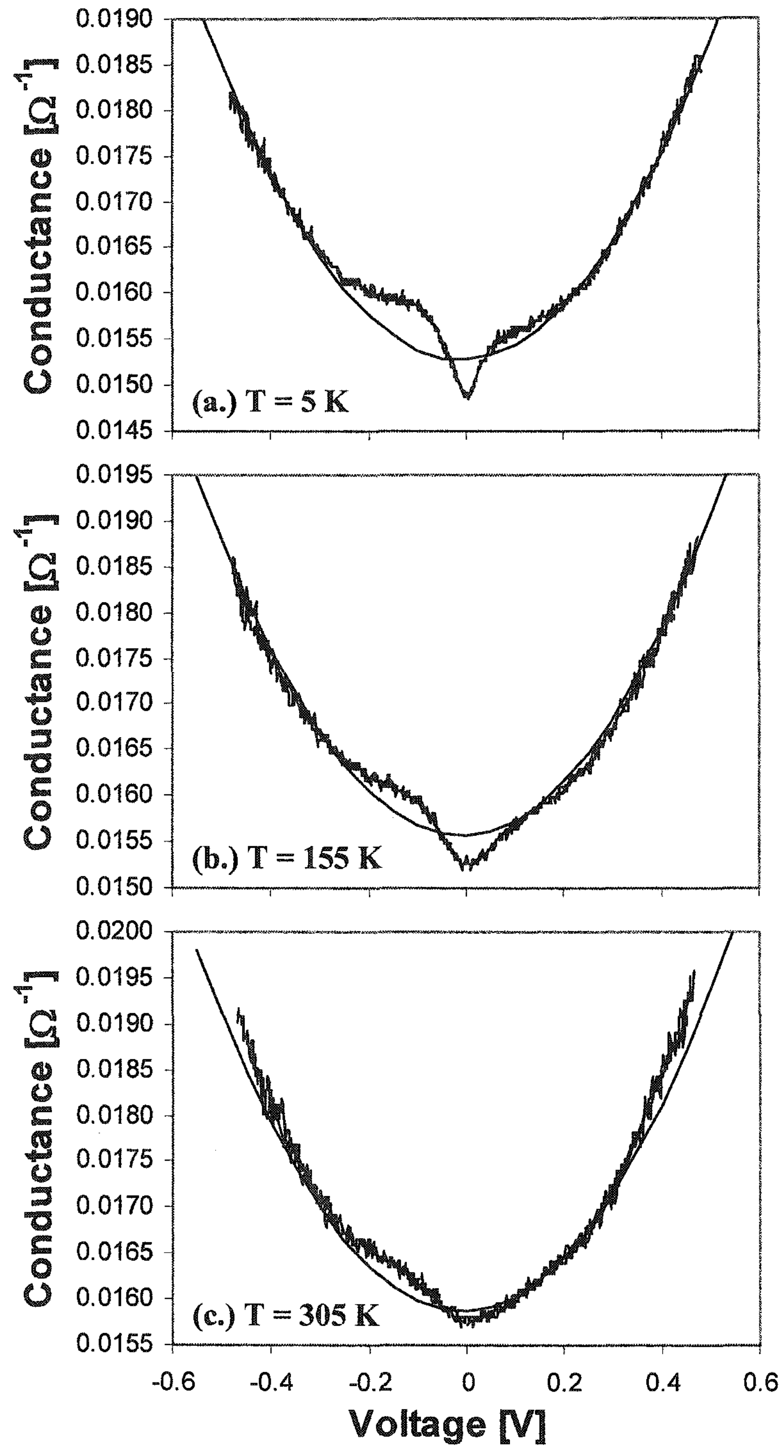

Figure 3. Parallel G-V dependence at (a.) T = 5 K, (b.) T = 155 K, and (c.) T = 305 K. The arms of dynamical conductance at higher temperatures can be reasonably reproduced by fitting dynamical conductance at 5 K to the BDR model and assuming the presence of second order voltage hopping conductance. At a temperature of 305 K, voltage dependent hopping terms contribute significantly to total conductance.

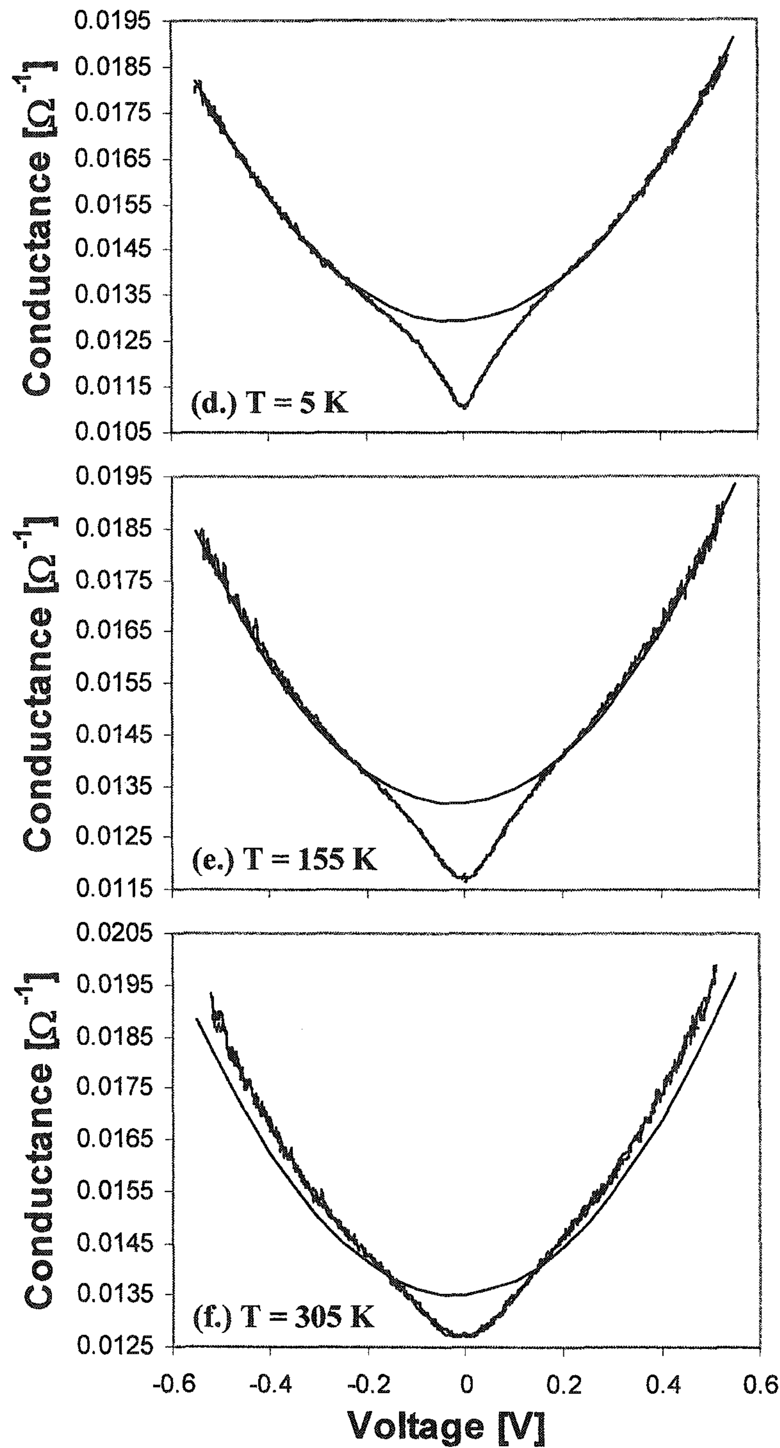

Figure 3. (continued) Anti-parallel G-V dependence at (d.) T = 5 K, (e.) T = 155 K, and (f.) T = 305 K. The arms of dynamical conductance at higher temperatures can be reasonably reproduced by fitting dynamical conductance at 5 K to the BDR model and assuming the presence of second order voltage hopping conductance. At a temperature of 305 K, voltage dependent hopping terms contribute significantly to total conductance.

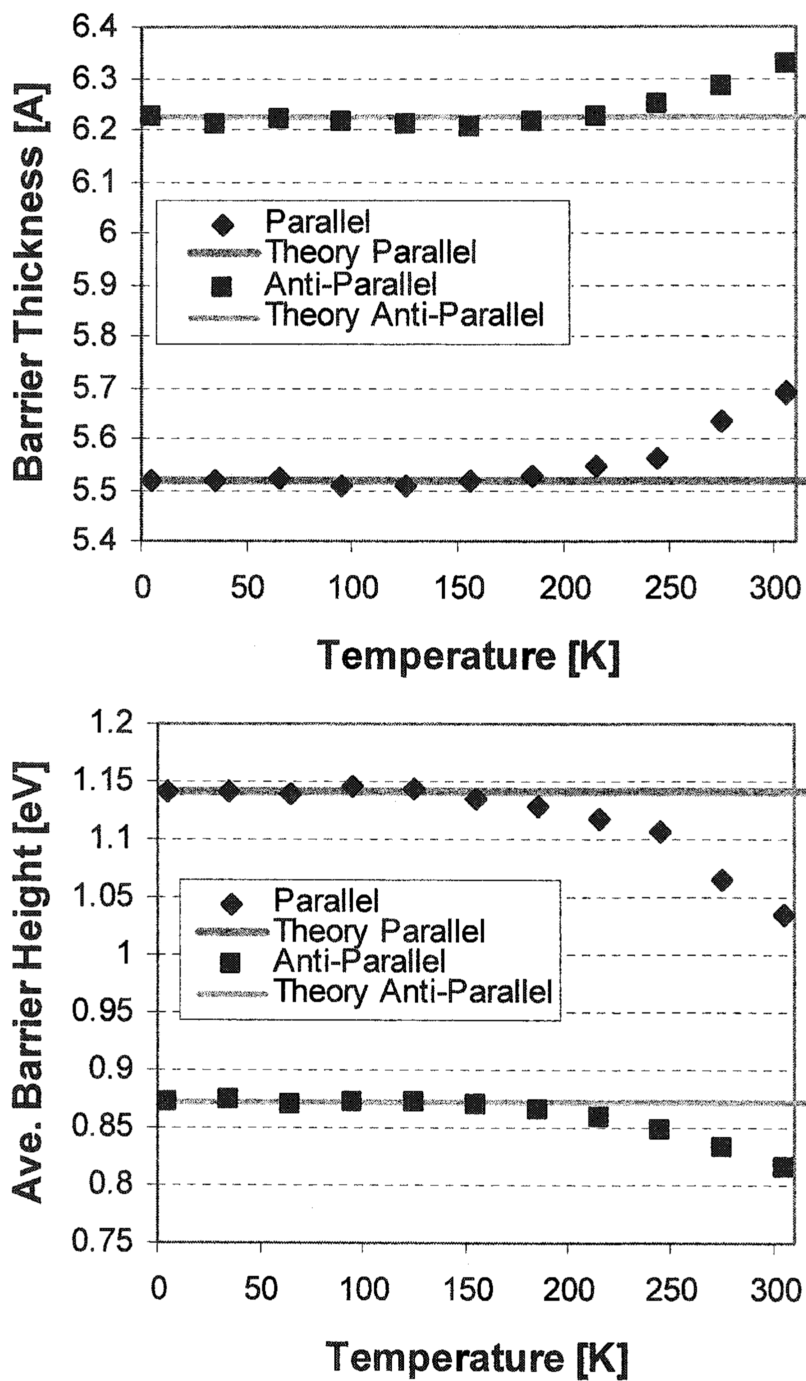

Figure 4. Effective barrier parameters as a function of temperature obtained by a direct fit to the BDR model. The deviation from constant values at elevated temperatures is related with the onset of voltage dependent hopping conductance.

Table 1. Barrier parameters extracted from direct fits to Stratton and BDR models. Last column shows the percentage contribution of hopping conductance at 305 K.

			Stratton param.		BDR param.				
barrier (Å)	RxA ($\Omega\mu m^2$)	magnetic orientation	t (Å)	Φ_{AVE} (eV)	t (Å)	Φ_{AVE} (eV)	Φ_{ASYM} (eV)	τ_2	$G_{SI}/G_P(V=0)$ T=305K
5.0	6.82	parallel	7.52	0.47	5.52	1.14	-0.09	2.3E-7	3.0%
		anti-parallel	8.28	0.38	6.22	0.87	-0.19		
5.25	9.76	parallel	7.62	0.53	5.46	1.35	-0.21	3.5E-7	2.9%
		anti-parallel	8.39	0.43	6.17	1.03	-0.32		
5.5	12.7	parallel	8.02	0.52	5.48	1.49	-0.28	2.7E-7	2.9%
		anti-parallel	8.89	0.42	6.14	1.16	-0.38		
15	7.9E6	parallel	18.52	1.00	11.56	2.86	0.32	8E-9	12.4%
		anti-parallel	20.09	0.85	12.34	2.51	0.98		

References

[1] W. F. Brinkman, R.C Dynes, J. M. Rowell, J. Appl. Phys. 89, 1915 (1970).

[2] R. Stratton, J. Phys. Chem. Solids 23, 1177 (1962); John G. Simmons, J. Appl. Phys. 35, 2655 (1964).

[3] Yun Li and Shan X. Wang, J. Appl. Phys. 91, 7950 (2002).

[4] E. L. Wolf, Principles of Electron Tunneling Spectroscopy (Oxford University Press, London, 1985).

[5] B. Oliver, Q. He, M. Tang, and J. Nowak, in preparation.

[6] C. H. Shang, J. Nowak, R. Jansen, and J. S. Moodera, Phys. Rev. B 58, R2917 (1998).

[7] L. I. Glazman and K. A. Matveev, Sov. Phys. JETP 67, 1276 (1988).

[8] Bryan Oliver Qing He, Xuefei Tang, Janusz Nowak, to appear in J. Appl. Phys. 94, (2003).

[9] Y. Xu, D. Ephron, and M. R. Beasley, Phys. Rev. B 52, 2843 (1995).

Two Breakdown Mechanisms in Ultra-Thin Alumina Barrier Magnetic Tunnel Junctions

A paper submitted to the Journal of Applied Physics

Bryan Oliver,[1] Gary Tuttle,[2] Qing He,[1] Xuefei Tang,[1] and Janusz Nowak[1]

[1]*Seagate Technology LLC, 7801 Computer Avenue South, Bloomington, MN 55435*

[2]*Microelectronics Research Center, Iowa State University, Ames, Iowa 50011*

Abstract

Two breakdown mechanisms are observed in magnetic tunnel junctions having an ultra-thin alumina barrier. The two breakdown mechanisms manifest themselves differently when considering large ensembles of nominally identical devices under different stress conditions. The results suggest that one type of breakdown occurs because of the intrinsic breakdown of a well-formed oxide barrier that can be described by the E model of dielectric breakdown. The other is an extrinsic breakdown related to defects in the barrier rather than the failure of the oxide integrity. The characteristic of extrinsic breakdown suggests that a pre-existing pinhole in the barriers grows in area by means of dissipative (Joule) heating and/or electric field across the pinhole circumference.

Introduction

Magnetic tunnel junctions (MTJs) are promising candidates for development of magnetic read heads for densities greater than 100 Gb/in^2. Before MTJ-based read heads can break through to a manufacturing stage, extensive tests involving a large ensemble of devices

across a wafer are needed in order to determine the reliability of these devices. Analysis of oxide breakdown is important for ultra-thin barrier MTJs in order to isolate the origin of the failure and indicate a course of optimization or remedy that is needed. Several key parameters in the study of oxide breakdown and the determination of breakdown mechanism are barrier thickness, junction area, substrate temperature, and dielectric lifetime under constant bias. While the last point was not practical for us to study, we instead used a current ramp technique from which a projection of the dielectric lifetime under low bias voltage can be extracted.[1,2,3,4]

As described earlier,[5] two breakdown mechanisms are observed in ultra-thin alumina barrier junctions: breakdown in which there is an abrupt decrease in the resistance at the maximum voltage across the barrier, whereas the other breakdown has a gradual decrease in resistance which can be easily identified at the maximum amplitude. These distinguishing characteristics suggest that devices that exhibit differing breakdown characteristics are inherently different from the beginning. We will demonstrate in this article that the origin of the observed breakdown mechanism is due to the presence of pinholes in the barrier.

To judge the presence of pinholes, one needs a dependable set of criteria. We have shown that all three of the Rowell criteria commonly used to judge the presence of pinholes in MTJs are insensitive to the presence of pinhole in ultra-thin alumina barriers.[6] We propose to include a statistical analysis of electrical breakdown to judge the pinhole presence using a large ensemble of nominally identical devices. While, unfortunately, the breakdown test is a destructive one, it can be used to assess the barrier quality by virtue of the observed breakdown mechanism. We will show that the measurements of devices that are experimentally observed to break abruptly provide evidence that suggests that the barrier

layer has suffered intrinsic dielectric breakdown of a well-formed oxide. The cause of intrinsic breakdown can be explained by the E model of dielectric breakdown,[7,8] which says that the dipole moment of a bond can interact with the applied field and be broken with finite probability. As for the devices observed to break gradually, the measurements support evidence that there is a pinhole, or for that matter many pinholes, present in the barrier layer that allow for ohmic conduction in parallel to the desired tunnel conduction. The cause of extrinsic breakdown can be interpreted in two ways: by the localized heating of the pinhole and/or the electric field across the pinhole circumference. In either case, the pinhole grows with increasing current when the junction is biased beyond the breaking point. The gradual breakdown is an extrinsic breakdown event related to the defects in the barrier rather than the failure of the oxide integrity.

Experiment

The examined tunnel stacks have an alumina barrier with the structure Ta(50Å)/PtMn(250Å)/CoFe(22Å)/Ru(9Å)/CoFe(22Å)/Al–ox/CoFe(10Å)/NiFe(25Å) /Ta(150Å) grown in-situ on a bottom electrode. The pinned layer is composed of a CoFe/Ru/CoFe trilayer that is antiferromagnetically coupled to the PtMn, whereas the free layer is a CoFe/NiFe bilayer. The substrate was an AlTiC wafer. Deep ultraviolet lithography was used to pattern sub-micron size devices. Metal layers were deposited using DC magnetron sputtering in an Ar plasma and the alumina barrier was formed by the natural oxidation of the aluminum metal layer that is nominally 4.75, 5.0, 5.25, and 5.5 Å. The actual thickness of the alumina layer has not been determined. We differentiate between the alumina barrier thickness by instead using the deposited thickness of aluminum metal.

However, for naturally oxidized alumina barrier, the thickness is approximately 1.28 greater than un-oxidized aluminum metal. This would yield an alumina barrier of 6.08, 6.40, 6.72, and 7.04 Å, respectively.

Sixty-four nominally identical junctions across a wafer were measured in each breakdown test. The devices are then separated into groups, intrinsic or extrinsic, based in the observed breakdown characteristic. The results displayed in the plots show the average of these groupings. Before a breakdown test is done, TMR versus RA was measured by biasing the junction at 20mV using constant voltage source.

For the majority of the breakdown experiments, the devices were biased in a single current ramp using a constant current source. A large current is chosen so to increase the bias voltage well beyond the barrier breaking point. A typical sweep begins at nominally 10mV, and then increases in ramp steps. Each current ramp has 150 total steps. R-H transfer curves were measured at each step in an external magnetic field of 1000 Oe. Some breakdown tests were done using a multiple ramp technique (see Figure 1), where the junction is ramped to a bias, measured at a 20mV constant voltage, then ramped to progressively higher and higher bias while returning to measure a reference at 20 mV constant voltage to determine the junction properties without any bias dependence. When this technique is utilized, the measurements at this 20 mV reference voltage are reported for the indicated applied stress voltage or current.

The breakdown test is done with a current ramp. This results in the voltage ramp speed (dV/dt) decreasing with increasing current because of the bias dependence of the junction resistance. However, the dV/dt decrease is not significant (note: the resulting change in model calculations is small) when considering devices breaking intrinsically.

Devices breaking extrinsically show much less bias dependence, and as such, the dV/dt can be considered almost constant up to the breaking point. Because of this, the average of this voltage ramp speed is reported in this work.

Results

In Figure 2, the area and thickness dependence on breakdown mechanism is presented. The data shown is the fraction of 64 nominally identical junctions breaking abruptly; devices breaking gradually make up the remainder. When comparing devices of at a junction area of 0.06 μm^2, it is clear that having a thicker barrier will increase the chance of the device breaking abruptly. There is a only about 9% chance to observe a device break abruptly when using 4.75 Å barrier, whereas increasing the barrier by only 0.75 Å to 5.5 Å this chance is dramatically increased by almost ten times to 88%! Similarly, for devices of equivalent thickness, increasing the junction area decreases the chance of observing abrupt breakdown. Increasing the junction area from 0.06 to 0.20 μm^2, the chance for seeing a device break abruptly increases from 88% to 70% at 5.5 Å. At 4.75 Å, no devices at all were observed to show abrupt breakdown at an area larger than 0.10 μm^2.

Figure 3 shows the area and thickness dependence on the breakdown voltage. Devices that show an abrupt decrease in resistance at the breaking point have large breakdown voltage compared to devices showing gradual change in resistance at breakdown. Furthermore, devices breaking abruptly show a strong dependence of the breakdown voltage on barrier thickness and junction area, whereas devices breaking gradually show a weak dependence. A MTJ with 4.75 Å barrier and 0.06 μm^2 area typically breaks abruptly around 600 mV. By increasing the barrier 0.75 Å, the breakdown voltage increases considerably to

an average of 850 mV. Similar junctions that break gradually show breakdown voltage of about 320 mV at 4.75 Å but increasing to only around 385 mV at 5.5 Å. By increasing the junction area from 0.06 to 0.2 μm^2 for the 5.5 Å barrier, the abrupt breakdown voltage decreases about 12% to an average of 760 mV. Similar devices breaking gradually show no significant dependence on the area.

In Figure 4, the voltage ramp speed dependence on the breakdown voltage is shown. By stressing similar groups of samples in which the voltage ramp speed was the only parameter varied, information of the dependence of the dielectric lifetime on the junction voltage can be obtained. The smallest area junctions (0.06 μm^2) were measured at room temperature to emphasize the distinction between abrupt and gradual breakdown. It is seen that devices which break abruptly have a strong dependence on the ramp speed, showing a decrease of about 50-60 mV when decreasing the voltage ramp speed by about 30 times. Conversely, devices that break gradually show no significant change with voltage-ramp speed. It is noteworthy to report the fraction of devices showing abrupt breakdown was not significantly influenced by voltage ramp speed. Fractions at each ramp speed for 5.5, 5.25, 5.0, and 4.75 Å are about 0.80, 0.46, 0.26, and 0.07, respectively, which is consistent with Figure 2. For 4.75 Å thickness, the tests at each ramp speed were repeated three times in order to have larger population of devices exhibiting abrupt breakdown.

Shown in Figure 5 is a plot of the breakdown voltage dependence on substrate temperature measured for each thickness. The experiment was done by heating the substrate chuck, holding all other parameters constant. The smallest area junctions (0.06 μm^2) were measured at the fastest ramp speed in order to emphasize the distinction between abrupt and gradual breakdown. It is seen that devices that break abruptly have a strong dependence on

the substrate temperature, which fits well in an Arrhenius plot. At each of the four thicknesses, the abrupt breakdown voltage drops by around 100mV when increasing the substrate temperature from room temperature to 110°C. Conversely, devices that break gradually have a weak dependence on the substrate temperature, showing a drop of around 10mV for the same temperature change. As with voltage ramp speed, the fraction of devices showing abrupt breakdown was not influenced by changing substrate temperature. Fractions at each temperature for 5.5, 5.25, 5.0, and 4.75 Å are about 0.81, 0.48, 0.26, and 0.08, respectively, which is consistent with Figure 2.

The graph in Figure 6 shows the TMR versus RA product for the twenty sets of sixty-four devices presented in Figure 1 and 2 measured before the breakdown test using a 20 mV constant bias voltage. RA products for 4.75, 5.0, 5.25, and 5.5 Å typically are in the range of 5-10, 10-20, 16-30, and 25-40 $\Omega\mu m^2$, respectively. Separating the results according to the breakdown characteristic reveals the TMR is correlated with the breakdown mechanism. Devices that break abruptly, regardless of barrier thickness, have TMR that is maximal, about 23.5%; we can say that its TMR is weakly dependent on the RA product. Conversely, devices that break gradually have TMR strongly dependent on RA product. Many factors can influence the observed TMR, such as the presence of pinholes, as will be discussed in the section on extrinsic breakdown.

Intrinsic Breakdown Analysis

The experimental observation of abrupt breakdown can be interpreted using the E model of intrinsic dielectric breakdown. As the dielectric is subjected to an electric field, the E model proposes[7] there is a net dipole moment induced which causes a bond distortion.

This field-induced strained bond is expected to introduce strong anharmonic coupling with the lattice. The anharmonic coupling allows the strained bonds to interact with thermal phonons, increasing the probability of breakdown of the dielectric. The intrinsic dielectric failure is thus associated with the physical properties of the oxide and its variation of structure and composition. As such, the intrinsic failure will occur at the weakest link in the barrier material. Applied stresses of electric field and temperature will accelerate the probability for dielectric breakdown.[7,8] The junction area will also affect this probability as the variations of the barrier material can become greater over larger areas.[2] Oepts et al. presented an analysis which concluded that the observed intrinsic dielectric breakdown of alumina barrier ferromagnetic tunnel junctions was well described with use of the E model.[1] These results were followed in agreement by Schmalhorst et al.[3]

Following in the analysis done by Oepts et al.,[1] if *F(t)* denotes the fraction of devices that break intrinsically after a time *t*, the breakdown probability density is defined as $p(t) = (dF/dt)/(1-F)$. In the E model, *p(t)* is defined as

$$p(t) = A\exp(V(t)/B), \qquad \text{Eq. 1}$$

where $V(t)=E(t)*t_B$ is the time dependent voltage for intrinsic breakdown with *E(t)* being the electric breakdown field and t_B as the barrier thickness. If no clear time dependence is assumed for p(t), $A \sim A_J * \exp(-E_A/kT)$ where A_J is the junction area, E_A is the activation energy for dielectric breakdown, and $B = kTt_B / a|qZ|$, where $a=2$ Å is the atomic spacing for Al_2O_3 and $Z=3$ for Al^{3+} ions. For experiments with dV/dt constant, an intrinsic failure *F(t)* can be given by

$$F(t) = 1 - \exp\left[- p(t)B\left(\frac{dV}{dt}\right)^{-1} + AB\left(\frac{dV}{dt}\right)^{-1}\right]. \qquad \text{Eq. 2}$$

The failure rate, which is the peak of *dF(t)/dt*, is found at

$$V_{MAX} = B\ln\left(\frac{dV}{dt}\frac{1}{AB}\right), \qquad \text{Eq. 3}$$

where V_{MAX} is the breakdown voltage observed at a voltage-ramp speed dV/dt.

We can roughly estimate the parameter B. For naturally oxidized aluminum, the thickness is approximately 1.28 greater than un-oxidized aluminum. This yields an oxidized barrier of 7.04, 6.72, 6.40, and 6.08 Å when starting with aluminum 5.5, 5.25, 5.0, and 4.75 Å, from which the estimated values of B for oxidized aluminum are respectively 0.0296, 0.0283, 0.0269, and 0.0256 V at room temperature. This can be compared to experimental values extracted from the slope of the breakdown voltage dependence on the voltage ramp speed. The measured values of B for 5.5, 5.25, 5.0, and 4.75 Å are respectively 0.0170, 0.0167, 0.0140, and 0.0117 V. It is clear the measured values of B scale with thickness of the barrier, where we find the oxide barrier thickness will be 4.04, 3.97, 3.33, and 2.78 Å, respectively when solving for the barrier thickness t_B from the equation for B. These results are around 43-61% of what we believe the oxide barrier thickness to be. Nonetheless, the model predictions of B are on the same order of the measured values. The parameter A is obtained by fitting the model in equation 3 to the data plot. These values of A extracted using the known ramp speed and the value for B given above; values of A for 5.5, 5.25, 5.0, and 4.75 Å are respectively 2.1×10^{-22}, 1.5×10^{-19}, 2.0×10^{-20}, 1.0×10^{-22} s^{-1}.

The activation energy of dielectric breakdown E_A can be extracted from the slope of breakdown voltage dependence of substrate temperature along with a known value for the

parameter A. We found values for E_A of 1.65, 1.69, 1.73, and 1.75 eV, respectively for aluminum thickness of 5.5, 5.25, 5.0, and 4.75 Å. These results suggest two important points. First, the physical mechanism governing the observation of abrupt breakdown is the same independent of thickness, as in the Arrhenius relationship there exists (within some experimental tolerance) one activation energy of dielectric breakdown. Second, the breakdown mechanism doesn't change with temperatures up to 110°C used to accelerate the breakdown.

For a time independent breakdown probability density p(t), the mean lifetime is given by

$$\tau_{1/2} = \frac{\ln(2)}{p(t)} \qquad \text{Eq. 4}$$

where $\tau_{1/2}$ is the time where 50% of devices have experienced breakdown. Using the values for parameters A and B, it is clear that breakdown is accelerated when using thinner and thinner barriers. From Figure 7, using the E model the estimated lifetime at a constant voltage bias of 0.47 V yields a lifetime of 103 years for 5.5 Å aluminum thickness. However, for thinner barriers of 5.25 Å, a bias of about 0.36 V is needed for to get the projected lifetime above 100 years, whereas 0.32 V is required for 5.0 Å or 4.75 Å barriers. These constant bias voltage numbers are approximately 50% of what the breakdown voltage is at the fastest voltage-ramp speed. Increasing this constant bias voltage by 10% will decrease the projected lifetime by a factor of 10.

Intrinsic breakdown is accelerated at higher temperatures as well. As seen in Figure 5, the temperature dependence of the intrinsic breakdown voltage follows an Arrhenius relationship, which is expected since $A \sim A_J * \exp(-E_A / kT)$. For 5.5 Å, this leads to a

projected lifetime of just 5.4 days when biased at 0.47 V at 110°C. Decreasing the constant bias voltage to 0.27 V, which is 58% of bias at room temperature, the projected lifetime at 110°C will return to about 102 years. Similarly, for thinner aluminum of 5.25, 5.0 and 4.75 Å, the bias voltage must be reduced below 50% the bias at room temperature in order to keep projected lifetimes around 100 years.

Scaling of the junction area has consequences on the breakdown voltage as seen in Figure 3 (as well as the breakdown mechanism, as seen in Figure 2). The parameter A is proportional to the junction area if the breakdown probability is independent of the location on the junction area. It has been proven[9] that if the breakdown sites are randomly distributed, F will scale with the junction area A_J of the device

$$\ln(-\ln(1-F_2)) - \ln(-\ln(1-F_1)) = \ln(A_{J2} / A_{J1}) \qquad \text{Eq. 5}$$

To verify the random character of the area distribution of breakdown sites, we analyzed the free layer reversal before and after intrinsic breakdown.[5] The value of H_I was observed to be very sensitive to the location of the breakdown site in the junction area. The value of H_I after breakdown was observed to shift by an amount that was dependent in the applied current amplitude and direction as well as the lateral position of the pinhole with respect to the magnetic field. This suggests that the breakdown event is not along the junction perimeter but instead is randomly distributed throughout the junction area.

Let us focus on 5.5 Å barrier devices since these have the largest number of devices that break intrinsically. From the figure of breakdown voltage dependence on junction area, it is seen that the breakdown voltage decreases 100 mV when increasing the junction area from 0.06 to 0.20 μm^2, a factor of 3.33. This contrasts the model prediction given by Equation 5, in which the breakdown voltage should decrease only 20 mV. So, for our

barriers, the model prediction under-estimates the values from actual data. This tells us the defect density is somewhat greater when the junction area is increased, which for ultra-thin barrier can be attributed to non-uniformity. In other words, the oxide is well formed, yet it has weak spots in it that cause the breakdown to be at a lower electric field than the model predicts. Consequently, the breakdown voltage in Figure 4 scales with the junction area as expected with the E model, but to a larger degree. Assuming the naturally oxidized aluminum metal is 1.28 times the thickness of un-oxidized aluminum, the electric breakdown field for 5.5 Å aluminum is approximately 12 MV/cm with junction area of 0.06 μm^2 but decreases to 11.3 MV/cm at junction area of 0.20 μm^2.

Scaling of barrier thickness has direct consequence on the breakdown voltage. At a junction area of 0.06 μm^2, decreasing the aluminum thickness in 0.25 Å steps decreases the electrical breakdown field to 10.8, 10.1, and 10.1 MV/cm at 5.25, 5.0, and 4.75 Å barriers. There is much less consequence in area scaling at these thicknesses. This result is unclear. Factors to be considered are incomplete oxidation, the non-uniformity of the deposition, and the substrate roughness. Optimization of each of these could improve the area and thickness dependence of the breakdown voltage. However, this could as well be attributed to the fact that the number of devices breaking intrinsically decreases much at these thicknesses, which doesn't allow many devices to be considered.

Extrinsic Breakdown Analysis

Devices in which the junction resistance breaks down gradually have a pinhole (or pinholes) in the barrier.[6,10,] These suffer extrinsic breakdown of an imperfect barrier. We propose that the results of devices breaking gradually can be explained by analysis of the

Joule heating effect in the pinhole. The pinhole is conductive relative to the insulating barrier, so it shunts the current. Localized heating of the pinhole will occur when the applied current stresses the junction beyond a critical voltage. After surpassing this critical voltage, the power dissipative heating effect is so large that the pinholes start to grow. However, the results can also suggest that during the pinhole growth it is rather a strong, localized electric field at the pinhole circumference that plays an important role. In either case, the result is the area of the tunnel resistor decreases, causing a decrease in both junction resistance as well as magnetoresistance. In theory, pinholes can be minimized by optimizing the deposition of the barrier material, the oxidation, the surface roughness of the substrate and underlying layers, and using ultra-high vacuum deposition equipment as well as high-class clean-room. This makes breakdown analysis of tunnel junctions an excellent tool for studying the influence of deposition and processing conditions.

Let us recall two observations: as shown in Figure 2, increasing the junction area and decreasing the barrier thickness leads to greater probability that the tunnel junction will exhibit gradual breakdown; from Figure 6 we see that devices which show gradual breakdown have always lower TMR. These results lead to the conclusion that devices that exhibit gradual breakdown indeed have a pre-existing pinhole or pinholes. Since the pinhole is conductive relative to the tunnel resistor, it shunts the current. A significant amount of current is conducted through the pinhole, which, when large enough, can influence the properties of the pinhole and the barrier around the perimeter of the pinhole. We must therefore consider the effect of this current shunting on the barrier.

To describe the extrinsic breakdown mechanism, let us examine a typical device having 5 Å barrier shown in Figure 8a. This device was first biased at 20 mV to examine its

initial resistance and TMR. Then, the breakdown test is initiated by stressing at progressively higher bias voltages. The transfer curve was re-measured after each stress measurement using a low bias of 20 mV to look for the onset of any permanent damage (see Fig. 1). Any permanent change in resistance or TMR can then be solely attributed to the stress voltage. This device when biased at 20 mV constant voltage has TMR = 15.68% and RA = 9.08 $\Omega\mu m^2$. As the applied voltage is increased higher and higher, the RA product is nearly constant until surpassing a threshold voltage of about 270 mV, where further increase of the voltage across the barrier results in the resistance gradually decreasing. Figure 8b shows the TMR response as a function of the junction resistance. We see that the TMR response decreases linearly with the effective RA product of the device, i.e., the TMR tracks the junction resistance. This process can be visualized as the growth of a pre-existing pinhole. With increasingly larger applied current, the pinhole area increases, which in turn causes the measured RA product to decrease. The increasing pinhole area shunts more and more current, which causes the TMR response to become smaller and smaller.

We can describe devices that exhibit extrinsic breakdown by a resistance model of a tunnel resistor in parallel with an ohmic short. We have earlier[10] described the effective RA product as

$$RA_{EFF}(x) = \frac{A}{\left(\frac{A-x}{RA_{INTRINSIC}}\right)+\left(\frac{x}{RA_{SHORT}}\right)} \qquad \text{Eq. 6}$$

where x is the area of the pinhole (or pinholes). It is noteworthy that by continuing the stress test well beyond the breaking point for this device, we can extrapolate the TMR to zero, where we can hypothesize that since the TMR is zero, the entire barrier is destroyed and is

now a gigantic pinhole. For this device, at TMR = 0, the RA product would be 0.8 $\Omega\mu m^2$. Since the TMR linearly tracks the resistance, the RA product of the pinhole is then 0.8 $\Omega\mu m^2$. For the junctions discussed here we will call this RA_{SHORT}. $RA_{INTRINSIC}$, i.e. the RA product of the device if there were no pinhole in the barrier, can be estimated by the following:

$$RA_{INTRINSIC} = \frac{TMR_{INTRINSIC}}{TMR_{EFF}(x)}\left[RA_{EFF}(x) - RA_{SHORT}\right] - RA_{SHORT} \qquad \text{Eq. 7}$$

For the devices that break intrinsically, the typical TMR is 23.5% (see Figure 7). Therefore, we just extrapolate TMR to 23.5% for the value of $RA_{INTRINSIC}$, which for this device is 13.25 $\Omega\mu m^2$. See Fig. 8b. With RA_{SHORT} and $RA_{INTRINSIC}$ known, the pinhole area can be estimated for any device given its junction area and low-bias resistance with a simple transformation of Eq. 6:

$$x = \frac{A \times RA_{SHORT}}{RA_{EFF}}\left(\frac{RA_{INTRINSIC} - RA_{EFF}}{RA_{INTRINSIC} - RA_{SHORT}}\right) \qquad \text{Eq. 8}$$

For a device that exhibits TMR(x) = 15.68 % and RA(x) = 9.08 $\Omega\mu m^2$ (measured at 20 mV bias), this tells us that the pinhole area is about 0.0018 μm^2 , which is around 3% of the junction area, from the beginning – before the breakdown process had begun.

Figure 9a shows the dependence of pinhole area on applied current. For currents smaller then 2 mA, the effective voltage on junction is small and the pinhole does not grow. When the effective voltage on the junction reaches a critical value, ~300 mV (~2.2 mA), the pinhole begins to grow. The growth of the pinhole is roughly proportional to the applied current and to the applied power. We can distinguish a change in the slope in Figure 9a around 3.2 mA of current. At that moment, the pinhole occupies 9% of junction area and

effective voltage on junction begins to increase gradually. At the end of the current sweep, which is 6 mA, the pinhole occupies 18% of junction area and effective voltage on junction is equal 330 mV. Knowing the pinhole area, we can calculate the density of power dissipated at the pinhole. Figure 9b shows how the power density dissipated at the pinhole varies with the applied current. About 120 mW/μm^2 is needed for continuous pinhole growth. As the pinhole gets larger, slightly larger power density is needed. The data suggests that the pinhole growth is driven by heat generated at the pinhole itself. However, 300 mV voltage corresponds to about 6 MV/cm electric field across the 5 Å barrier. One can easily imagine that it is not the Joule heating effect, but rather a strong, localized electric field at the pinhole circumference that plays an important role during the pinhole growth. To answer the question what is the role of electric field during the pinhole growth we estimated the power dissipated at the pinhole and electric field across the barrier during the pinhole growth. Table 1 shows the dependence of these parameters on barrier thickness. Both breakdown voltage and effective RA for pinhole scale with Al thickness; however, the electric field across the barrier and the power density at the pinhole are almost constant with thickness. From this data, we cannot conclude what is causing the pinhole growth – the heat dissipation or the electric field.

The extrinsic breakdown mode was not observed to depend on the junction area, substrate temperature, and voltage-ramp speed (Figures 3-5). The only parameter on which the extrinsic breakdown voltage depends is barrier thickness. For 5.5 Å and 4.75 Å thick barriers, the extrinsic breakdown is around 380 mV and 320 mV, respectively. However, the small influence of voltage ramp speed and temperature on breakdown voltage should not be interpreted as an indicator of no stress induced wear-out, i.e. infinite lifetime at bias voltage

less than the extrinsic breakdown voltage. While in this study extrinsic breakdown is dependent on the power dissipated and/or the electric field at the pinhole, these factors may only dominate in the stress regime studied here. The stress factors of voltage and temperature may still prove significant outside this regime. If this were the case, stress induced wear-out as suggested by the E model would be considered a competing breakdown process to the heat-dissipative breakdown and/or electric field process for tunnel junctions with an imperfect barrier. To get a better understanding of extrinsic breakdown of a barrier with a pinhole, this study would need to be extended to include a much wider range of both voltage ramp speed and temperature than what was done here.

Conclusion

We have demonstrated that the two breakdown mechanisms observed in ultra-thin alumina barrier MTJ reveal themselves in contrasting ways by studying parameters of barrier thickness, junction area, voltage-ramp speed, and substrate temperature. It was found that the observed breakdown mechanism is related directly to the presence of pinholes in ultra thin alumina barrier.

MTJs showing an abrupt decrease in resistance at the breaking point are observed to fail due to intrinsic dielectric breakdown of a well-formed oxide that can be described using the E model. The stress of electric field and temperature were found to accelerate the breakdown of the junctions. Consequences of scaling the junction area and the barrier thickness can be associated with the physical properties of the oxide and its variation of structure and composition. These variations can possibly be attributed to incomplete oxidation, deposition non-uniformity, and substrate roughness.

MTJs showing a gradual decrease in the resistance at the breaking point were determined to fail due to an extrinsic breakdown mechanism caused by pinhole presence. We were able to estimate the pinhole area and the pinhole growth during the breakdown event using two resistor model of MTJ and extrapolating existing data to two extreme situations: when the MTJ has no pinhole and when the MTJ is completely covered by a gigantic pinhole. Extrinsic breakdown weakly depends on the stress factors that effect intrinsic breakdown: voltage-ramp speed and external temperature. Instead, we found that the power density at the pinhole and/or the electric field across the barrier are the main stress factors causing the pinhole to grow. To make projections of device lifetime, we need detailed knowledge about pinhole growth kinetics. At voltages much lower than the extrinsic breakdown voltage, the pinholes are stable, which demonstrates the potential use of ultra-thin barriers in tunneling hard drive sensors. From a microscopic point of view, ultra-thin barriers will always have pinholes (or at least atomic defects) and we should consider them as a new "composite" material in which the structure needs to be very precisely known and controlled.

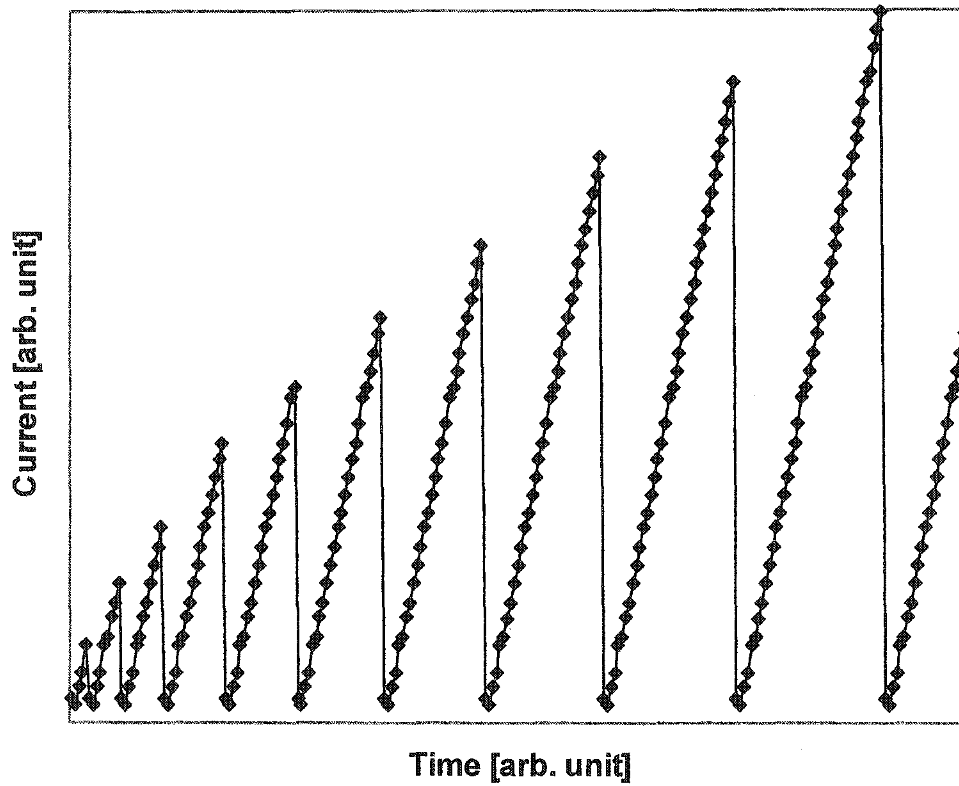

Figure 1. Multiple ramp tests used for study of the MTJ breakdown. After each progressively higher stress, the junction is measured at constant 20 mV bias.

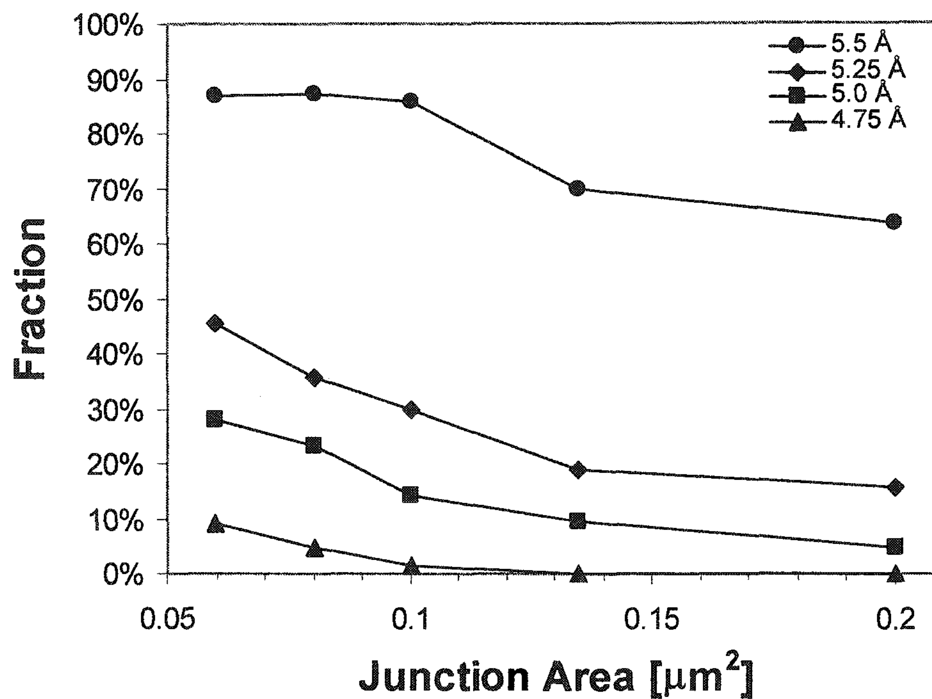

Figure 2. Dependence of thickness and area on the fraction of devices that break down abruptly. Each point represents a fraction 64 nominally identical MTJs. 5.5 Å (●), 5.25 Å (◆), 5.0 Å (■), 4.75 Å (▲).

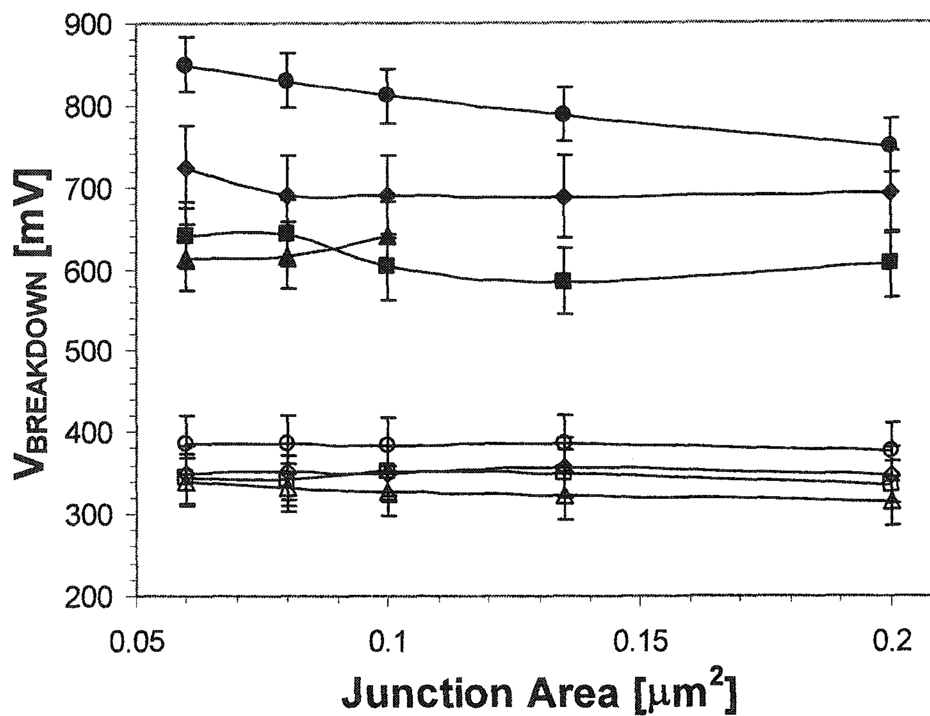

Figure 3. Breakdown voltage dependence on the area and thickness. Each point is an average. 5.5 Å (●), 5.25 Å (◆), 5.0 Å (■), 4.75 Å (▲). Solid markers represent abrupt breakdown; hollow markers represent gradual breakdown. Error bars indicate standard deviations.

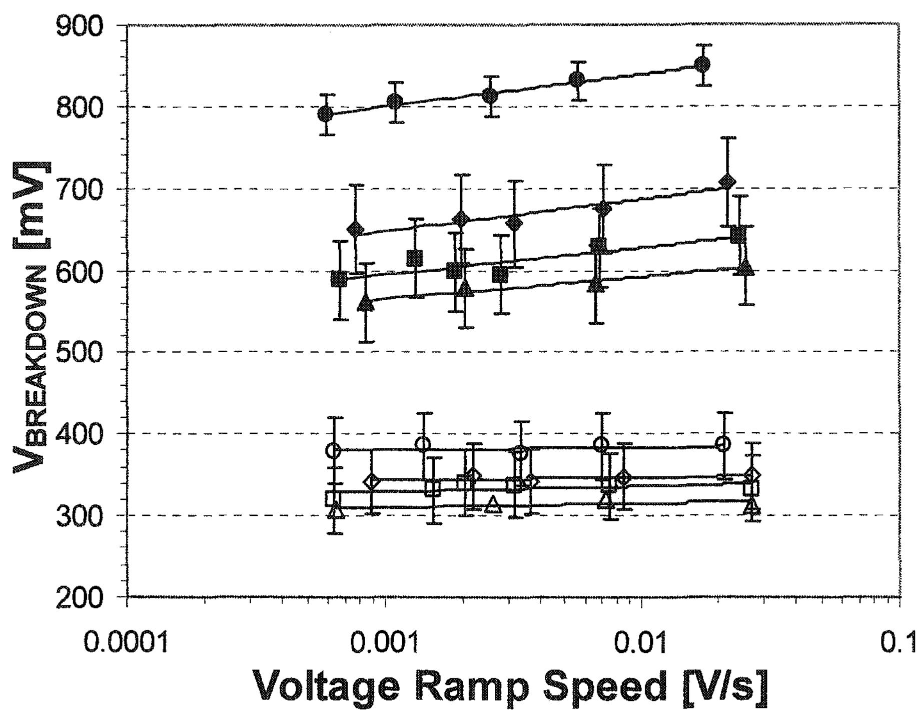

Figure 4. Breakdown voltage dependence on voltage ramp speed. Each marker represents an average. 5.5 Å (●), 5.25 Å (◆), 5.0 Å (■), 4.75 Å (▲). Solid markers represent abrupt breakdown; hollow markers represent gradual breakdown. The junction area is 0.06 μm^2. Error bars indicate standard deviations.

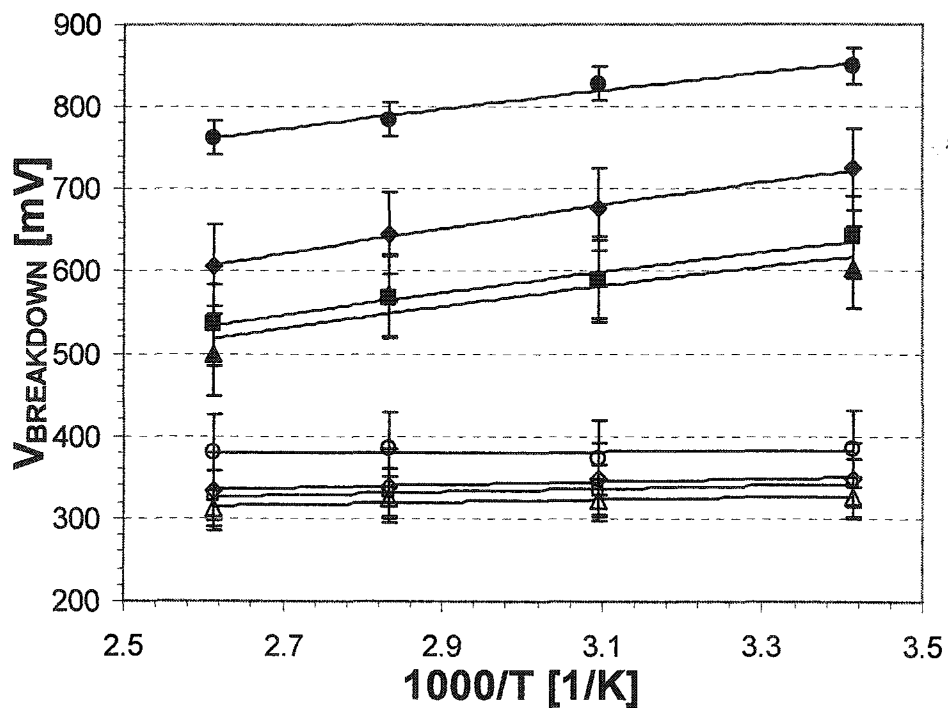

Figure 5. Breakdown voltage dependence on substrate temperature. Each point is an average. 5.5 Å (●), 5.25 Å (◆), 5.0 Å (■), 4.75 Å (▲). Solid markers represent abrupt breakdown; hollow markers represent gradual breakdown. The junction area is 0.06 μm^2. Error bars indicate standard deviations.

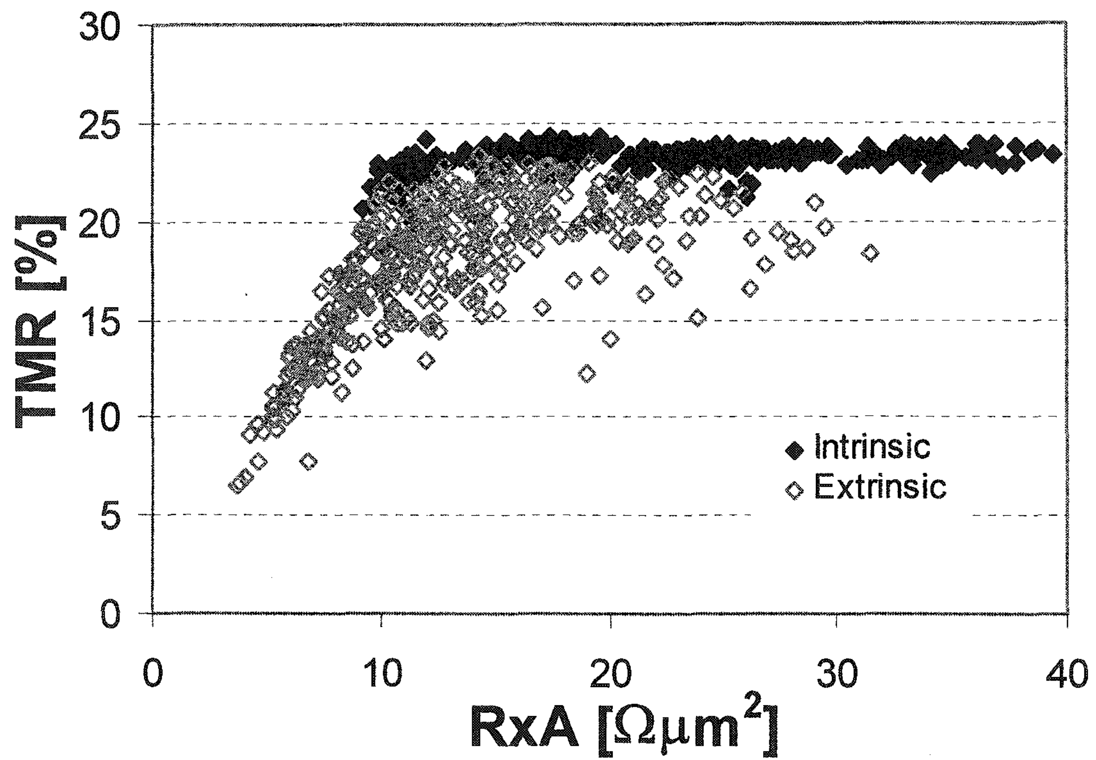

Figure 6. TMR vs. RA product of 1280 devices. The devices are separated according to the breakdown mechanism. Solid markers represent intrinsic (abrupt) breakdown; hollow markers represent extrinsic (gradual) breakdown.

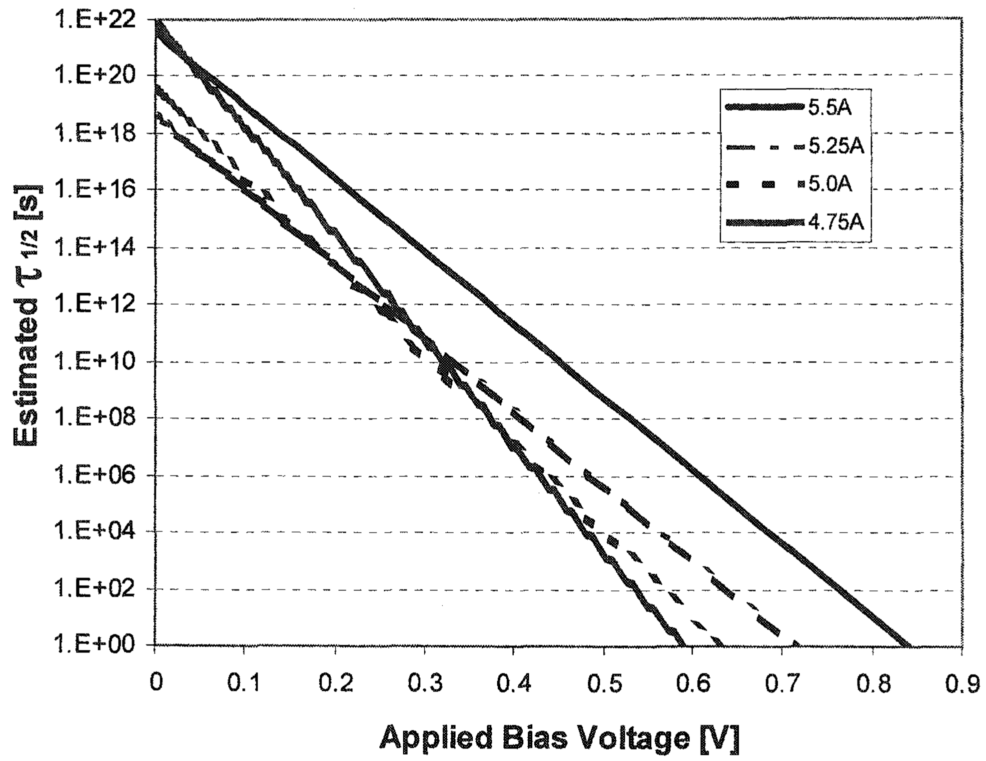

Figure 7. Estimated lifetime of devices exhibiting intrinsic breakdown using the E model of dielectric breakdown.

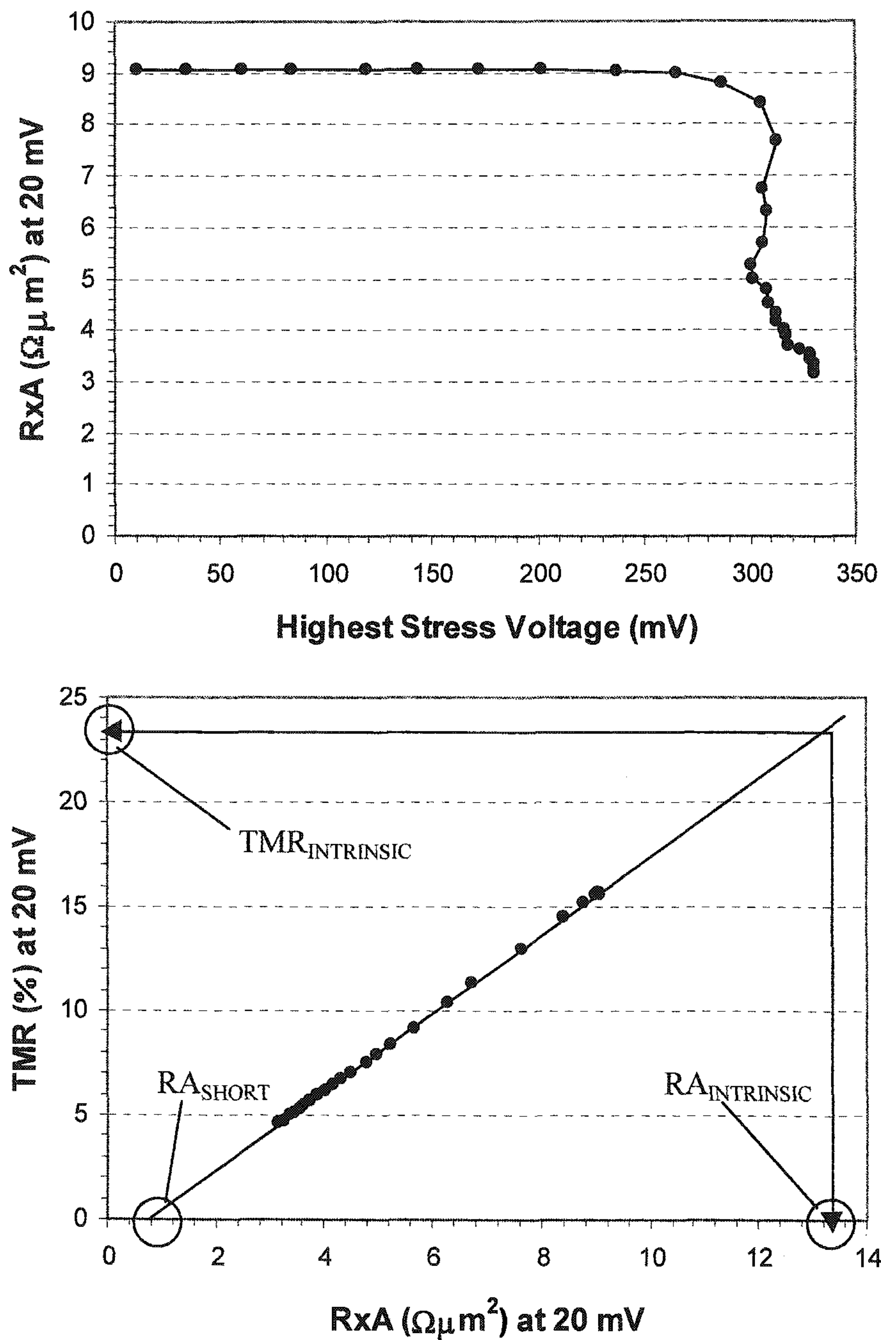

Figure 8. Multiple ramp test of the device that breaks down extrinsically beginning at 270 mV. Both RA products for pinhole and tunnel barrier can be estimated from extrapolation.

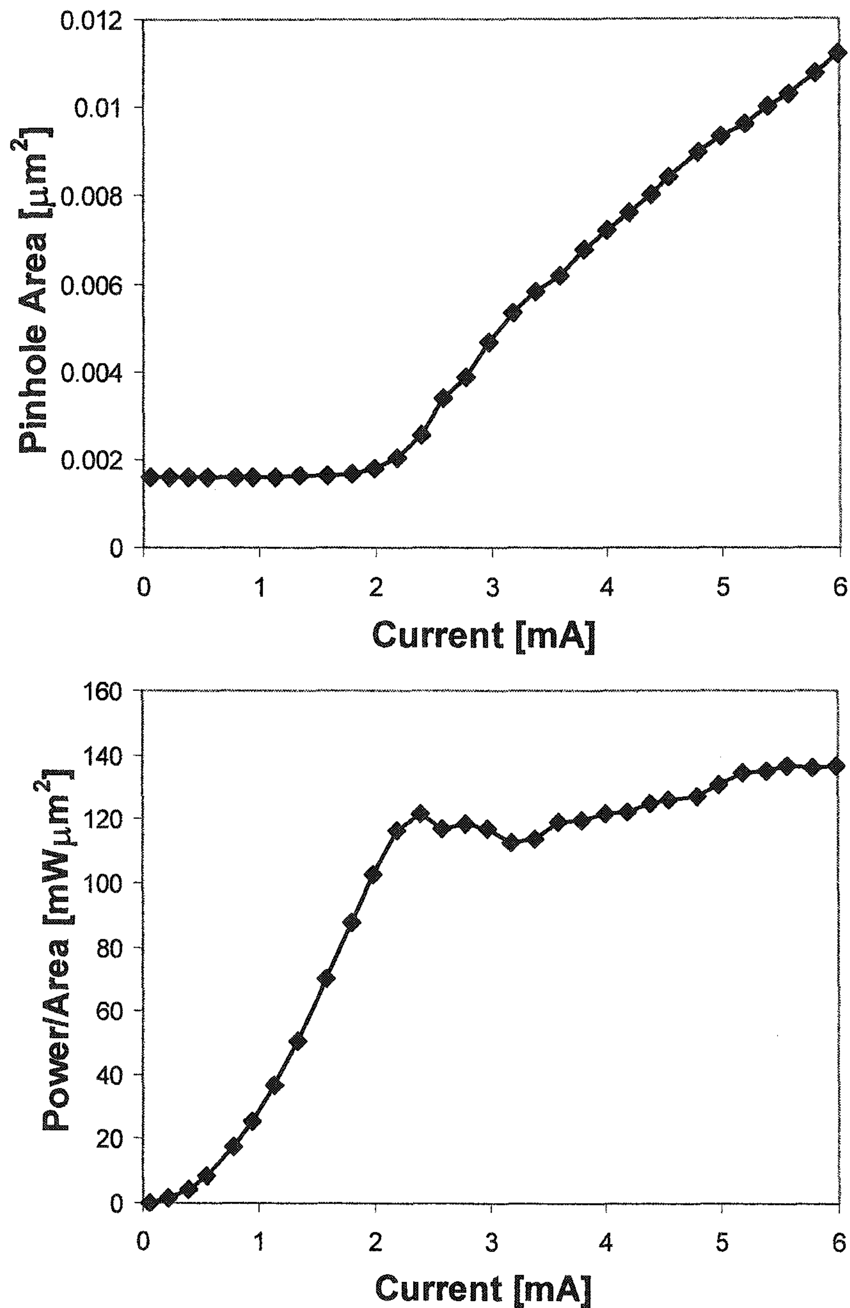

Figure 9. Extrinsic breakdown of the device during multiple ramp constant current sweep from 0.06 to 6 mA (see Fig. 1). A pre-existing pinhole occupies 3% of the junction area and begins to grow with current greater than 2 mA. A power density of 120mW/μm^2 at the pinhole is needed for continuous pinhole growth.

Table 1. Estimated pinhole RA and breakdown voltage scale with aluminum thickness, whereas the electric field and dissipative power heating are mostly constant.

thickness [Å]	RxA_S [$\Omega\mu m^2$]	$V_{Breakdown}$ [mV]	$E_{Breakdown}$ [MV/cm]	$V_{Breakdown}^2/RxA_S$ [$mW/\mu m^2$]
4.75	0.69	321	6.8	154
5	1.18	335	6.7	96
5.25	1.32	347	6.6	93
5.5	1.41	379	6.9	104

References

[1] W. Oepts, H. J. Verhagen, W. J. M. de Jonge, and R. Coehorn, Appl. Phys. Lett. 73, 2363 (1998).

[2] K. Shimazawa, N. Kasahara, J. J. Sun, S. Akari, H. Morita, and M. Matsuzaki, J. Appl. Phys 87, 5194, (2000)

[3] J. Schmalhorst, H. Brückl, M. Justus, A. Thomas, G. Reiss, M. Vieth, G. Gieres, and J. Wecker, J. Appl. Phys. 89, 586 (2001).

[4] D. Rao, K. Sin, M. Gibbons, S. Funada, M. Mao, C. Chien, and H.-C. Tong, J. Appl. Phys. 89, 7362 (2001).

[5] B. Oliver, Q. He, X. Tang, and J. Nowak, J. Appl. Phys. 91, 4348 (2002).

[6] Bryan Oliver, Qing He, Xuefei Tang, and Janusz Nowak, to appear in J. Appl. Phys. 94, (2003).

[7] J. W. McPherson and H. C. Mogul, J. Appl. Phys. 84, 1513 (1998).

[8] M. Kimura, International Reliability Physics Proceedings (IEEE, Piscataway, NJ, 1997), p. 190.

[9] D. R. Wolters and J. F. Verwey, *Instabilities in Silicon Devices* (Elsevier, Amsterdam, 1986).

[10] H. Kikuchi, M. Sato, and K. Kobayashi, Fujitsu Sci. Tech. J. 37, 183 (2001).

General Conclusions

Ultra-thin alumina barrier magnetic tunnel junctions (MTJs) were examined. Such thin barriers can be imperfect and have pinholes. Examination of bias and temperature dependence of the MTJs supports a model of two resistors in parallel: one a tunnel magnetoresistor, the other an Ohmic resistor. Moreover, the results indicate that in addition to the tunneling conductance, hopping conductance through the barrier is present. It was found that even in the presence of pinholes, the dynamic conductance exhibits a parabolic dependence on the applied voltage as well as an insulating-like resistance dependence on temperature. These results suggest commonly used criteria for judging the presence of pinholes in tunnel junction barriers is insufficient and unreliable.

The presence of pinholes in the ultra-thin barrier is of major concern, as is the reliability of the barrier layer under stress. Two types of breakdown mechanisms are observed in ultra-thin barrier MTJs. It was found that the breakdown mechanism is an indicator of the barrier quality. Junctions showing an abrupt change in resistance at the breaking point have relatively large breakdown voltage ($V_B > 0.6$ V) and fail due to intrinsic breakdown of a well-formed oxide that follows the *E* model of dielectric breakdown. On the other hand, the breakdown of junctions showing a gradual decrease in resistance at the breaking point occur at a much lower voltage ($V_B \sim 0.3$-0.4 V), which is related to the presence of pinholes in the barrier. Current concentrated at the pinhole after breakdown generates a strong, circular magnetic field, which curls the local magnetization in the free-layer around the pinhole. This makes the free-layer reversal very sensitive to the location of the breakdown point in the junction area. Thus, the presence of pinholes can have strong

implications on the parametric margins of the ultra-thin barrier MTJ for read sensor applications. It is proposed to include a statistical analysis of breakdown mechanisms to determine the presence of pinholes in ultra-thin barrier MTJs.

Acknowledgements

"I'm the luckiest man in the world, now that Lou Gehrig's dead."

--Homer Simpson, The Simpsons

While I normally wouldn't say this, when I look back at everything in my life, I have to admit that I am one of the luckiest people around, if not the luckiest. While some aspects of my life have proved to be difficult, overall, things have gone relatively well for me. Honestly, the only reason I believe things happened the way they have is because there have been lots of good people around at the right time who helped make my success possible. I wouldn't be in this position today without their help.

There are many people to list here. If I forgot someone, it is strangely a reflection of having been in school most of my life, which in doing so has turned me into a careless idiot, especially these last few years. So, in no particular order:

- Thanks to Song Xue of Seagate Technology for believing in me. I honestly couldn't believe it when I got the job. Song is the reason I was able to do research for this Dissertation at Seagate.

- Janusz Nowak was an invaluable contributor to this Dissertation. Most of what I know about magnetic tunnel junctions, Janusz happily took his own time out of the busy days to teach me.

- Mike Tang, who has been my Seagate manager, and Qing He, a fellow engineer, both contributed significantly to the stack development for this Dissertation as well as lending helpful advice in my research.

- Thanks to Gary Tuttle, who served as my major professor, not only for his patient guidance and suggestions for this Dissertation, but for the fundamental discussions as well.

- Vik Dalal and Joe Shinar for their contributions as part of my committee. In addition, for their invaluable support when I worked with them years ago, when they taught me most of what I know about thin film growth and characterization.

- Art Pohm and John Snyder for their contributions as part of my committee.

- All the people I worked with previously at the Microelectronics Research Center at Iowa State University, in particular Karl Erickson, Jason Herrold, Tim Maxson, Curtis Sell, and Jon Kavanaugh. Besides the laughs, they were also there to help mask my inherent stupidity by answering any of the questions I had.

- My friends and co-workers at Seagate Technology, far too many people to list out here.

- My old friends, who I never get to visit, but who helped keep me from going insane at one point in my life or another: Sean Collins, Ed Szymanski, Jenny Stoner, Reuben Waters, and Steve Zieser (who quite oddly prefers to be called Fatty). Also, my old friend, Helice Agria, who helped me out when I needed her. I may not smile a lot, but when I do, it's usually because in my mind I'm thinking of the fun times I had with these people. I really don't know what I would have done without them.

- The creators and the writers of the Simpsons, Space Ghost Coast to Coast, and the Larry Sanders Show, the makers of Mountain Dew, and the designers of Goldeneye for the Nintendo 64.

- Thanks to Robert and Darlene Berchtold for giving me the best place in Ames to live while going to ISU.

- Thanks to my parents, Gary and Mary, for encouraging me and for working very hard to make sure the doors of college were open for me, as well as my brothers, Jason and Chad, and my sister, Dena, for their understanding and unwavering patience with me. They each provided enormous help.

Iowa State University
Thesis/Dissertation Abstract

(Submit two copies with the final copies of your thesis or dissertation)

Student Name: *Type your complete name as shown on your title page* Bryan Kent Oliver

Thesis/Dissertation Title: *Type the title of your thesis/dissertation using the same wording and capitalization as on your title page* Ultra-thin alumina barrier magnetic tunnel junctions

Major Professor(s): Gary Tuttle

Ultra-thin alumina barrier magnetic tunnel junctions (MTJs) were examined. Such thin barriers can be imperfect and have pinholes. Examination of bias and temperature dependence of the MTJs supports a model of two resistors in parallel: one a tunnel magnetoresistor, the other an Ohmic resistor. Moreover, the results indicate that in addition to the tunneling conductance, hopping conductance through the barrier is present. It was found that even in the presence of pinholes, the dynamic conductance exhibits a parabolic dependence on the applied voltage as well as an insulating-like resistance dependence on temperature. These results suggest commonly used criteria for judging the presence of pinholes in tunnel junction barriers is insufficient and unreliable.

The presence of pinholes in the ultra-thin barrier is of major concern, as is the reliability of the barrier layer under stress. Two types of breakdown mechanisms are observed in ultra-thin barrier MTJs. It was found that the breakdown mechanism is an indicator of the barrier quality. Junctions showing an abrupt change in resistance at the breaking point have relatively large breakdown voltage ($V_B > 0.6$ V) and fail due to intrinsic breakdown of a well-formed oxide that follows the E model of dielectric breakdown. On the other hand, the breakdown of junctions showing a gradual decrease in resistance at the breaking point occur at a much lower voltage (V_B

~ 0.3-0.4 V), which is related to the presence of pinholes in the barrier. Current concentrated at the pinhole after breakdown generates a strong, circular magnetic field, which curls the local magnetization in the free-layer around the pinhole. This makes the free-layer reversal very sensitive to the location of the breakdown point in the junction area. Thus, the presence of pinholes can have strong implications on the parametric margins of the ultra-thin barrier MTJ for read sensor applications. It is proposed to include a statistical analysis of breakdown mechanisms to determine the presence of pinholes in ultra-thin barrier MTJs.